P-07-140

Oskarshamn site investigation

Borehole KLX17A

Microcrack volume measurements and triaxial compression tests on intact rock

Lars Jacobsson
SP Technical Research Institute of Sweden, Borås, Sweden

June 2007

Svensk Kärnbränslehantering AB
Swedish Nuclear Fuel
and Waste Management Co
Box 5864
SE-102 40 Stockholm Sweden
Tel 08-459 84 00
+46 8 459 84 00
Fax 08-661 57 19
+46 8 661 57 19

ISSN 1651-4416
SKB P-07-140

Oskarshamn site investigation

Borehole KLX17A

Microcrack volume measurements and triaxial compression tests on intact rock

Lars Jacobsson
SP Technical Research Institute of Sweden, Borås, Sweden

June 2007

Keywords: Rock mechanics, Microcrack volume, Hydrostatic compression test, Triaxial compression test, Elasticity parameters, Stress-strain curve, AP PS 400-06-113.

Abstract

Hydrostatic compression tests and subsequent trixial compression tests have been carried out on 6 specimens of intact rock from borehole KLX17A in Oskarshamn. Moreover, the density and porosity of further 6 specimens were determined. The volume of microcracks, originating from stress relaxation and mechanical effects from the core drilling, was estimated by analysing the volumetric response during the hydrostatic compression tests. The specimens were packed into water tight bags right after the field sampling in order to preserve the natural water content. The porosity measurements and the mechanical tests were carried out at this moisture condition. The density was first determined at natural moisture condition and after drying.

The cylindrical specimens were taken from drill cores at three depth levels ranging between 255–256 m, 437–438 m and 635–636 m borehole length. The sampled rock type of all specimens was Ävrö granite. The microcrack volume, elastic properties, represented by the Young's modulus and the Poisson ratio, and the compressive strength were deduced from the mechanical tests. The specimens were photographed before and after the mechanical testing.

The density of the specimens had a mean value of 2,710 kg/m^3 at natural moisture content and 2,706 kg/m^3 after drying. The mean value of the measured porosity was 0.39%. The estimated microcrack volume was in the range 0.011–0.048%.

Two confining pressure levels were used, 10 and 50 MPa, and the peak values of the axial compressive stress were in the range 292.6–580.1 MPa. The elastic parameters were determined at a load corresponding to 50% of the failure load and it was found that Young's modulus was in the ran 65.1–72.7 GPa with a mean value of 69.0 GPa. The Poisson ratio was in the range of 0.30–0.37 with a mean value of 0.33. It was seen from the mechanical tests that the material in the specimens responded in a brittle way.

Sammanfattning

Hydrostatiska kompressionsprov och efterföljande triaxiella kompressionsprov har utförts på 6 stycken provobjekt av intakt berg från borrhål KLX17A i Oskarshamn. Vidare bestämdes densiteten och porositeten hos ytterligare 6 prover. Mikrosprickvolymen, härrörande från spänningsavlastning och mekaniska effekter från kärnborrningen, uppskattades genom att analysera den volymetriska responsen under de hydrostatiska kompressionsproven. Proverna packades in i vattentäta påsar direkt efter provtagningen för att bevara det naturliga fukttillståndet. Porositetsmätningarna samt de mekaniska provningarna utfördes med detta fukttillstånd. Densiteten bestämdes hos proverna vid naturligt fukttillstånd och efter torkning.

De cylindriska proven har tagits från borrkärnor vid tre djupnivåer mellan 255–256 m, 437–438 m och 635–636 m borrhålslängd. Bergarten hos alla prover var Ävrögranit. Från de mekaniska provningarna bestämdes mikrosprickvolymen och de elastiska egenskaperna, representerade av elasticitetsmodulen och Poissons tal. Provobjekten fotograferades såväl före som efter de mekaniska proven.

Densiteten hos proverna hade ett medelvärde på 2 710 kg/m^3 med naturlig fukthalt samt 2 706 kg/m^3 efter torkning. Medelvärdet hos den uppmätta porositeten var 0,39%. Den uppskattade mikrosprickvolymen var mellan 0,011–0,048 %.

Två olika celltryck användes vid triaxialproven, 10 och 50 MPa, och toppvärdena för den axiella kompressiva spänningen låg mellan 292,6–580,1 MPa. De elastiska parametrarna bestämdes vid en last motsvarande 50 % av topplasten vilket gav en elasticitetsmodul mellan 65,1–72,7 GPa med ett medelvärde på 69,0 GPa. Poissons tal var mellan 0,30–0,37 med ett medelvärde på 0,33. Vid belastningsförsöken kunde man se att materialen i provobjekten hade ett sprött beteende.

Contents

1 Introduction

Density and porosity determination, microcrack volume measurements and triaxial compression tests have been carried out on drill core specimens sampled from the borehole KLX17A in Oskarshamn, Sweden, see map in Figure 1-1. These tests belong to one of the activities performed as part of the site investigation in the Oskarshamn area managed by the Swedish Nuclear Fuel and Waste Management Co (SKB) /1/. The tests were carried out in the material and rock mechanics laboratories at the department of Building Technology and Mechanics at Technical Research Institute of Sweden (SP), former Swedish National Testing and Research Institute (before January 2007).

Borehole KLX17A is a drilled borehole with a total length of c 700 m, which has a vertical angle of 60 degrees and is oriented in the 17 degree direction (N017O).

The controlling documents for the activity are listed in Table 1-1. Both Activity Plan and Method Description are SKB's internal controlling documents, whereas the Quality Plan referred to in the table is an SP (The Swedish National Testing and Research Institute) internal controlling document.

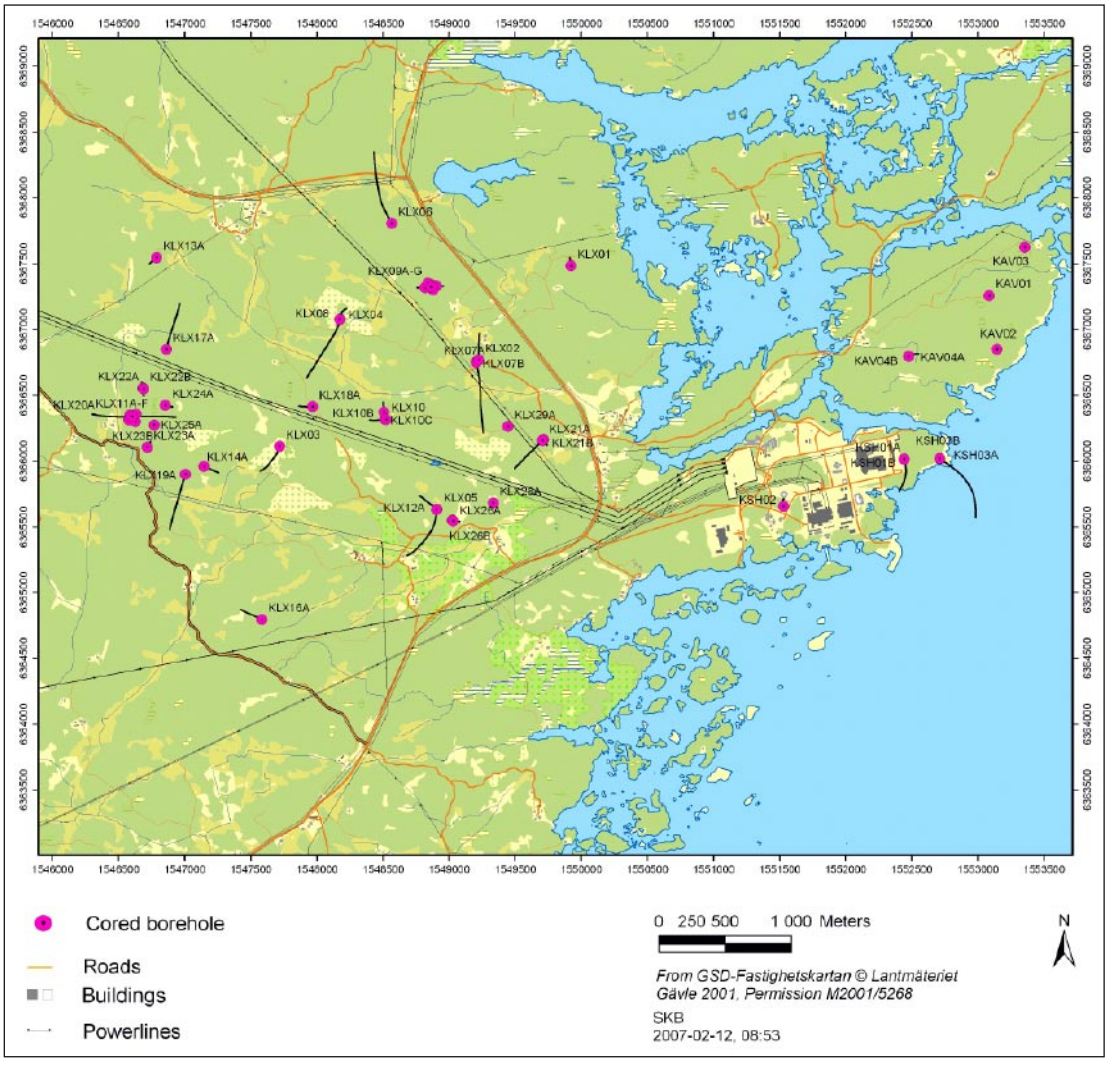

Figure 1-1. *Map showing cored boreholes and their projections at the Oskarshamn candidate area in February 2007.*

Table 1-1. Controlling documents for performance of the activity.

Activity Plan	Number	Version
Mätning av microsprickors töjningsvolym vid treaxliga tryckförsök – KLX17A	AP PS 400-06-113	1.0
Method Description	**Number**	**Version**
Determining density and porosity of intact rock	SKB MD 160.002	3.0
Triaxial compression test for intact rock	SKB MD 190.003	3.0
Quality Plan		
SP-QD 13.1		

The method description SKB MD 160.002, which is based on the ISRM suggested method /2/, was followed for the porosity and density determinations. The method description SKB MD 190.003, which is based on the ISRM suggested methods /3, 4/, was partly followed for sampling and for the triaxial compression tests. As to the measurements of microcrack volume there is no known standardized test method. Moreover, SKB has no method description for measurements of microcrack volume. A method was developed to determine the microcrack volume in laboratory on intact rock core specimens that can be carried out prior to triaxial tests, cf. /5/. The method is further described below and in Section 4.6.

SKB supplied SP with rock cores which arrived at SP in November 2006 and were tested during December 2006 and January 2007. Cylindrical specimens were cut from the core and selected based on the preliminary core logging with the strategy to primarily investigate the properties of Ävrö granite (501044).

The core parts were packed into sealed plastic bags directly after sampling in order to preserve their natural water content and opened right before the specimen preparation. Each of the core parts was split into one specimen for the density and porosity determination and one specimen for the mechanical tests. The porosity was determined based on the natural water content. The dry density and the density at natural water content were determined.

The natural water content was kept during the mechanical testing. Moreover, the specimens were photographed before and after the mechanical testing.

The measurement of microcrack volume was conducted by analysing the volumetric response of the specimens during hydrostatic compression. The test procedure was earlier used by e.g. Jacobsson /5/, Brace /6/ and Walsh /7/.

The compression tests with axial deformation control were carried out after the hydrostatic compression tests. The axial ε_a and circumferential strain ε_φ together with the axial stress σ_a were recorded during the test. The strains were recorded by means of strain gauges. The peak value of the axial compressive stress σ_c was determined at each test. Furthermore, two elasticity parameters, Young's modulus E and Poisson ratio v, were deduced from the tangent properties at 50% of the peak load. Diagrams with the volumetric and crack volumetric strain versus axial stress are reported. These diagrams can be used to determine crack initiation stress σ_i and the crack damage stress σ_d, cf. /8, 9/.

2 Objective

One purpose of the testing was to determine the volume of microcracks and the porosity on specimens in laboratory.

The in situ porosity is used when radionuclide transport properties in the rock mass are modeled. There is no established method to determine the in situ porosity in field. Porosity determined on drill core specimens in laboratory has been used instead in the computations. The specimens in laboratory have experienced a stress relaxation and mechanical stressing during the drilling operation. This results in a development of microcracks which causes an increase of the apparent porosity. Results from the radionuclide transport simulations displays a discrepancy to values that have been predicted based results from in situ experiments. A hypothesis is that the discrepancy in the simulation is caused by using apparent porosity from laboratory measurements instead of the in situ porosity. An estimate of the in situ porosity can be obtained by subtracting the volume of microcracks in the porosity values from laboratory measurements

The second part of the testing is carried out in order to determine the elastic properties, represented by Young's modulus and the Poisson ratio and the compressive strength of cylindrical intact rock cores at different constant confining pressures.

The results from the tests are going to be used in the site descriptive rock mechanics model, which will be established for the candidate area selected for site investigations at Oskarshamn.

3 Equipment

3.1 Specimen preparation

A circular saw with a diamond blade was used to cut the specimens to their final lengths. The surfaces on the specimens aimed for the mechanical tests were grinded after cutting in a grinding machine in order to achieve a high-quality surface for the axial loading that complies with the required tolerances. The measurements of the specimen dimensions were made with a sliding calliper. Furthermore, the tolerances were checked by means of a dial indicator and a stone face plate. The specimen preparation is carried out in accordance with ASTM 4543-01 /10/.

3.2 Density and porosity measurements

The specimens and the water were weighed using a scale for weight measurements. A thermometer was used for the water temperature measurements. A heating chamber was used for drying the specimens. Further information of the equipment can be found in e.g. /11/. The expanded uncertainty for respective method with covering factor 2 (95% confidence interval) is ± 4 kg/m^3 for determination of wet density and ± 0.09% for determination of the porosity.

3.3 Deformation measurements and data acquisition

Metal foil strain gauges were used for the deformation measurements. It is found in the literature /12/ that a number of factors have to be considered when resistive metal foil strain gauges are used to determine material deformation during hydrostatic compression tests. The most important factor is the quality of the adhesive layer. Ideally the adhesive layer must be thin with an even thickness and with good bonding characteristics. Moreover, the adhesive layer must be free from air inclusions. The results can be more or less distorted if all these things are not fulfilled. Lateral pressure acting on the strain gauge will produce a small error on the strain readings which is approximately proportional to the acting pressure, see e.g. /12, 13/.

The gauge length must be many times larger than the grain size in the rock material in order to capture a homogenised response. Strain gauges with a gauge length of 20 mm were used. The selection of a proper adhesive is important as it must have good bonding characteristics on rock and must not be negatively affected by the presence of moisture. Lau and Chandler /14/ found that acrylic adhesive was the best working adhesive among various tested adhesives in conjunction with strain gauge measurements on wet rock during tests in a triaxial compression test device. We have therefore chosen a two-part metha-acrylate adhesive in the tests.

Test on aluminium reference specimens were carried out in order to develop a method to properly mount the strain gauges with an adhesive layer that is thin and with an even thickness and to investigate the pressure sensitivity. This investigation is described in /5/.

The data acquisition was made with a HBM MGCplus unit equipped with amplifier modules ML38-AP03 and ML10B-AP03 for the strain gauge channels. Each of the strain gauges was connected to a Wheatstone bridge with a sense connection for temperature compensation. Moreover, the load and pressure signals were also sampled with the HBM MGCplus unit.

3.4 Mechanical testing

The mechanical tests were carried out in a servo controlled testing machine specially designed for rock tests, see Figure 3-1. The system consists of a load frame, a hydraulic pump unit, a controller unit and various sensors. The communication with the controller unit is accomplished by special testing software run on a PC connected to the controller. The load frame is characterized by a high stiffness and is supplied with a fast responding actuator, cf. the ISRM suggested method /3/. Furthermore, the sensors, the controller and the servo valves are rapidly responding components. The machine is equipped with a pressure vessel in which the specimens are tested under a confinement pressure. A thin rubber membrane is mounted on the specimen in order to seal the specimen from the oil that is used as the confinement medium, cf. Figure 3-1.

The hydrostatic compression tests were carried out by letting pressurized oil act around the specimen where a pressure transducer registered the pressure. In the triaxial tests, the axial load is determined using a load cell, which is located inside the pressure vessel and has a maximum capacity of 1.5 MN. The uncertainty of the load measurement is less than 1%. The strain gauges measured both the axial and circumferential deformations in the tests.

The specimens were photographed with a 4.0 Mega pixel digital camera at highest resolution and the photographs were stored in a jpeg-format.

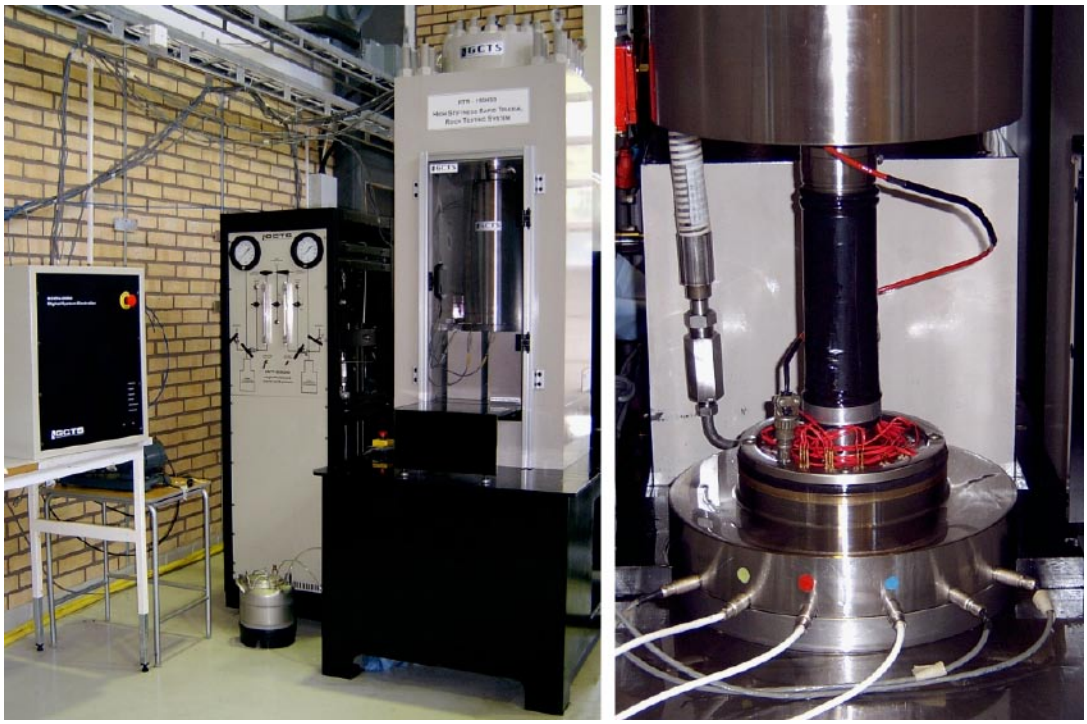

Figure 3-1. *Left: Digital controller unit, pressure cabinet with cell pressure intensifier and oil reservoir inside, and the load frame with closed cell (pressure vessel). Right: Bottom of the cell is lowered. The specimen is instrumented and ready for inserting in the cell.*

4 Execution

The determination of the density and porosity of the specimens were mainly made in accordance with the method description SKB MD 160.002 (SKB internal controlling document). This includes determination of density in accordance to ISRM /2/ with the exception that no water saturation was carried out. The microcrack volume measurements were carried out according to the method used by Brace /6/. The method description SKB MD 190.003 (SKB internal controlling document) was followed in large, but with a modified procedure regarding the triaxial compression test. The ISRM suggested method /3/ was instead followed for the triaxial compression tests in which strain gauges were used using instead of displacement transducers for the deformation measurements.

A check-list was filled in successively during the work in order to confirm that the different specified steps had been carried out. Moreover, comments were made upon observations made during the mechanical testing that are relevant for the interpretation of the results. The check-list form is an SP internal quality document.

4.1 Description of the specimens

The rock type characterisation was made according to Stråhle /15/ using the SKB mapping system (Boremap). The identification marks, upper and lower sampling depth (Secup and Seclow) and the rock types are shown in Tables 4-1 to 4-2.

Table 4-1. Specimen identification, sampling level (borehole length) and rock type for specimens aimed for density and porosity measurements (based on the Boremap mapping).

Identification	Adj Secup (m)	Adj Seclow (m)	Rock type/occurrence
KLX17A-80-1	256.01	256.22	Ävrö granite (501044)
KLX17A-80-2	255.81	256.01	Ävrö granite (501044)
KLX17A-80-4	437.35	437.69	Ävrö granite (501044)
KLX17A-80-5	437.69	437.95	Ävrö granite (501044)
KLX17A-80-7	635.76	636.04	Ävrö granite (501044)
KLX17A-80-8	636.04	636.31	Ävrö granite (501044)

Table 4-2. Specimen identification, sampling level (borehole length) and rock type for specimens aimed for mechanical tests (based on the Boremap mapping).

Identification	Adj Secup (m)	Adj Seclow (m)	Rock type/occurrence
KLX17A-115-1	256.01	256.22	Ävrö granite (501044)
KLX17A-115-2	255.81	256.01	Ävrö granite (501044)
KLX17A-115-4	437.35	437.69	Ävrö granite (501044)
KLX17A-115-5	437.69	437.95	Ävrö granite (501044)
KLX17A-115-7	635.76	636.04	Ävrö granite (501044)
KLX17A-115-8	636.04	636.31	Ävrö granite (501044)

4.2 Density and porosity measurements

The density of the specimens was determined at natural water content and after drying. Moreover, the porosity was determined based on measurements at the natural water content and at dry condition. An overview of the activities for the density and porosity determinations is shown in the step by step description in Table 4-3.

4.3 Preparation of specimens for mechanical tests

The specimens were cut to a prescribed length and the end surfaces of the specimens aimed for the mechanical testing were in addition grinded in order to comply with the required shape tolerances. Density measurements were carried out in the specimens having natural water content. The specimens were put in plastic bags after the density determination in order to preserve the natural moisture content.

The microcrack volume measurements are based on measuring and interpreting the volumetric response during hydrostatic compression tests. The deformations are measured by means of strain gauges. Six strain gauges, three in the axial direction and three in the circumferential direction, were mounted at mid height of the specimens. A coating was applied on the strain gauges as a mechanical protection. The specimens were tested right after the coating had been set.

Care has been taken to preserve the moisture up to testing. However, it has to be taken in account that some moisture have evaporated despite of this.

An overview of the activities during the specimen preparation is shown in the step by step description in Table 4-4.

Table 4-3. Activities during the density and porosity determinations.

Step	Activity
1	The specimens were cut according to the marks on the rock cores to a thickness of about 25 mm.
2	The specimens were weighed in tapwater with their natural water content. The temperature of the water was 19.7°C and the density 998.3 kg/m^3
3	The specimens were surface dried with a towel and weighed.
4	The density of the specimens having natural water content was determined.
5	The specimens were dried in a heating chamber for six days at 105°C.
6	The specimens were transported to a desiccator for cooling.
7	The dry density and porosity based on the natural water content were determined.

Table 4-4. Activities during the preparation of specimens for the mechanical tests.

Step	Activity
1	The drill cores were marked where the specimens are to be taken.
2	The specimens were cut to the specified length according to markings and the cutting surfaces were grinded.
3	The tolerances were checked: parallel and perpendicular end surfaces, smooth and straight circumferential surface.
4	The diameter and height were measured three times each. The respective mean value determines the dimensions that are reported.
5	The density at natural water content was determined and the specimens were repacked into plastic bags.

4.4 Mechanical tests

The specimen was placed inside the pressure cell between platens and sealed using a thin rubber membrane. Oil surrounded the specimen except under the lower platen as the platen was fixed to the cell bottom. This set-up yields an isotropic loading. Tests with two different load sequences were conducted. Type 1: Loading from 0.1–50 MPa, hold at 50 MPa for 15 minutes and unload 50–0.1 MPa and hold for 15 minutes. Type 2: Loading from 0.1–50 MPa, hold at 50 MPa for 5 minutes, loading from 50–100 MPa, hold for 5 minutes, unload 100–50 MPa, hold for 5 minutes, and unload 50–0.1 MPa and hold for 5 minutes. The pressure rate was 10 MPa/min during both loading and unloading during the tests except when testing specimen 8, where the loading rate 2 MPa/min was used instead.

The triaxial compression tests were carried out after the microcrack volume measurements using axial displacement control.

An overview of the activities during the mechanical testing is shown in the step by step description in Table 4-5.

Table 4-5. Activities during the mechanical tests. The steps 1–9 concern the microcrack volume measurements whereas the steps 10–14 concern the triaxial compression tests.

Step	Activity
1	Digital photos were taken on each specimen prior to the testing.
2	The specimen was put in testing position and centred between the loading platens.
3	A rubber membrane was mounted on the specimen and strain gauges were connected to the Wheat stone bridges.
4	The triaxial cell was closed and filled with oil whereby a cell pressure of 0.1 MPa is applied. The frame piston is positioned such that it will have a gap in the sperical joint to the upper loading platen.
5	The strain gauge channels were calibrated by means of a shunt resistance.
6	The sampling started and the cell pressure was ramped up to a pressure level of 50 MPa with a given constant rate. The pressure was hold at constant at 50 MPa at a given time.
7	Step 7 is only for the tests with a maximum pressure of 100 MPa (type 2).
	The pressure was ramped from 50 MPa to 100 MPa with a given constant rate. The pressure was hold at constant at 100 MPa at a given time.
8	Step 8 is only for the tests with a maximum pressure of 100 MPa (type 2).
	The pressure was ramped from 100 MPa to 50 MPa with a given constant rate. The pressure was hold at constant at 50 MPa for a short time (approximately 2–3 min).
9	The pressure was ramped from 50 MPa to 0.1 (0) MPa with a given constant rate. The pressure was hold at constant at the unloaded state for a given time.
10	The frame piston was brought down into contact with the specimen with a force corresponding to a deviatoric stress of 1 MPa. The cell pressure was then raised to the specified level and at the same time keeping the deviatoric stress constant.
11	The loading was started with axial displacement rate of the piston of 0.41 mm/min.
12	The test was stopped immediately after the axial peak load was rached.
13	The oil pressure was brought down to zero and the oil was poured out of the cell. The cell was opened and the specimen removed.
14	Digital photos were taken on each specimen after the mechanical testing.

4.5 Data handling

The test results were exported as text files from the test software and stored in a file server on the SP computer network after each completed test. The main data processing, in which the microcrack volume and elastic modulii were computed and the peak stress was determined, has been carried out in the program MATLAB /16/. Moreover, MATLAB was used to produce the diagrams shown in Section 5.2. The summary of results in Sections 5.1 and 5.3 with tables containing mean value and standard deviation of the different parameters and diagrams was provided using MS Excel. MS Excel was also used for reporting data to the SICADA database.

4.6 Analyses and interpretation

As to the definition of the different result parameters we begin with the axial stress σ_a, which is defined as

$$\sigma_a = \frac{F}{A}$$

where F is the axial force acting on the specimen, and A is the specimen cross section area. The pressure vessel (triaxial cell) filled with oil is pressurized with a cell (confining) pressure p. This implies that the specimen, located inside the pressure vessel, becomes confined and attains a radial stress σ_r equal to the confining pressure p. The (effective) deviatoric stress is defined as

$$\sigma_{dev} = \sigma_a - \sigma_r$$

The stresses during hydrostatic compression is $\sigma_a = \sigma_r = p$ (i.e. $\sigma_{dev} = 0$). The peak value of the axial stress during a test is representing the triaxial compressive strength σ_c, for the actual confining pressure used in the test, see the results presentation.

The strain measurements were carried out using strain gauges. The strain gauges are sensitive to lateral pressure. The lateral pressure sensitivity was previously investigated and quantified, cf. /5/. The measurement error made during a lateral pressure has two contributions which have to be accounted for. First, the lateral pressure acting on a strain gauge mounted on a plane surface was found to yield an underestimation of the strain results in the range of 22–34 micro-strain at a lateral pressure of 50 MPa with the current set-up. A second superposed effect was observed on strain gauges mounted on a convex single-curved surface with the curvature in the direction of the measuring grid. This effect was estimated to increase the measured strain value about 17.5 microstrain at lateral pressure of 50 MPa. Moreover, it was found that the amount of deviation was linearly proportional to the acting lateral pressure.

The strain data have been adjusted by using the findings above. Three strain gauges denoted AV, BV and CV, respectively, are measuring the axial strain at a 120 degrees division at mid height of the specimen. The correction of the vertical strain gauges (AV, BV and CV) are made according to

$$\varepsilon_{AV,corr} = \varepsilon_{AV} + C_{lat} \cdot p$$

for AV and similar for BV and CV, where ε_{AV} is the strain value of strain gauge AV obtained from measurements, p is the cell (confining) pressure which is equal to the lateral pressure and the constant $C_{lat} = 0.56$ microstrain/MPa was determined in /5/. Similarly, three strain gauges denoted AH, BH and CH, respectively, are measuring the circumferential strain at mid height of the specimen, with a division of 120 degrees. A correction of both the lateral pressure as stated above and due to the effect of curvature has to be made in this case. The correction in this case becomes

$$\varepsilon_{AH,corr} = \varepsilon_{AH} + C_{lat} \cdot p - C_{curvature} \cdot p$$

for AH and similar for BH and CH, where ε_{AH} is the strain value of strain gauge AH obtained from measurements and the constant $C_{curvature} = 0.35$ microstrain/MPa is obtained from /5/.

The axial and radial strains are represented by the mean values of respectively set of strain gauges as

$$\varepsilon_a = (\varepsilon_{AV,corr} + \varepsilon_{BV,corr} + \varepsilon_{CV,corr}) / 3 \quad (1)$$

and

$$\varepsilon_r = \varepsilon_\varphi = (\varepsilon_{AH,corr} + \varepsilon_{BH,corr} + \varepsilon_{CH,corr}) / 3 \quad (2)$$

The volumetric strain ε_{vol} is given as

$$\varepsilon_{vol} = \varepsilon_a + 2\varepsilon_r \quad (3)$$

Furthermore, the tangent bulk compliance β is defined as

$$\beta = d\varepsilon_{vol} / dp$$

The initial response during hydrostatic compression tests yields a non-linear response. For low porosity rock, the non-linearity is related to mainly closing of microcracks, cf. /7/. The deformation becomes approximately linear when the microcracks are closed and the deformations at this stage are associated with closing of natural pores and compression of the bulk material. With this view in mind, the microcrack volume strain ε_{MC} is computed as, cf. /7/,

$$\varepsilon_{MC} = \varepsilon_{vol,max} - \beta_{max}\, p_{max}, \quad (4)$$

where $\varepsilon_{vol,max}$ and p_{max} refer to values at 50 MPa in this investigation. The bulk compliance β_{max} were evaluated at $p = p_{max}$ (in the interval 48.0 – 49.6 MPa) at the unloading curve after further compression due to the creep deformations representing a compressed material as in situ. The principal stages of deformation during the hydrostatic compression test and the definition of the microcrack volume is visualised in Figure 4-1. In addition, the volumetric strain at 20 MPa pressure, denoted $\varepsilon_{vol,20}$, was determined as the mean value of the volumetric strain obtained at loading and at unloading. The level 20 MPa was chosen as it is in the same order as the in situ rock stresses in the two boreholes. The value of $\varepsilon_{vol,20}$ can be used to relate the to magnitude of volumetric deformations as they are in situ, with consideration of the microcrack volume strain ε_{MC}.

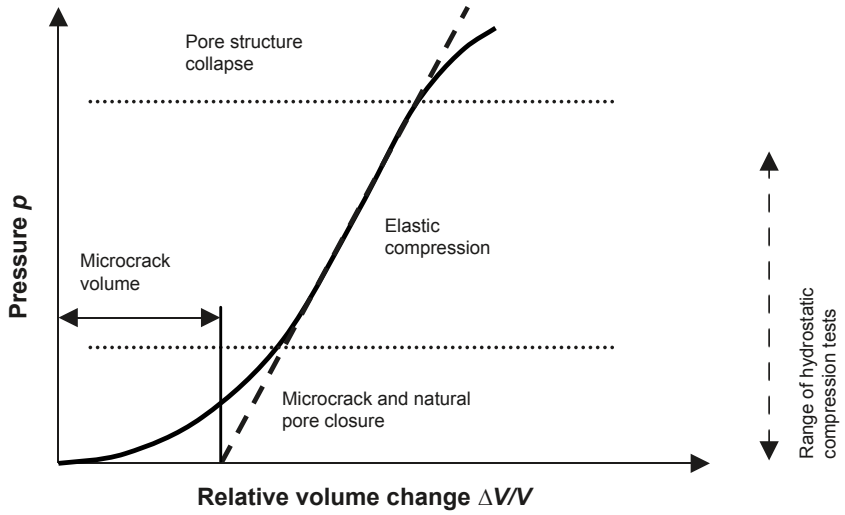

Figure 4-1. *Deformation phases during the hydrostatic compression test. The pore structure collapse will occur at very high pressures for a low porosity rock. The definition of the microcrack volume is shown.*

The stresses and the strains are defined as positive in compressive loading and deformation, respectively. The elasticity parameters are defined by the tangent Young's modulus E and tangent Poisson ratio ν as

$$E = \frac{\sigma_a(0.60\sigma_c) - \sigma_a(0.40\sigma_c)}{\varepsilon_a(0.60\sigma_c) - \varepsilon_a(0.40\sigma_c)}$$

$$\nu = -\frac{\varepsilon_r(0.60\sigma_c) - \varepsilon_r(0.40\sigma_c)}{\varepsilon_a(0.60\sigma_c) - \varepsilon_a(0.40\sigma_c)}$$

The tangents were evaluated with values corresponding to an axial load between 40% and 60% of the axial peak stress σ_c.

A closure of present microcracks will take place initially during confinement and axial loading. Development of new microcracks will start when the axial load is further increased and axial stress reaches the crack initiation stress σ_i. The crack growth at this stage is as stable as increased loading is required for further cracking. A transition from a development of microcracks to macro cracks will take place when the axial load is further increased. At a certain stress level the crack growth becomes unstable. The stress level when this happens is denoted the crack damage stress σ_d, cf. /8, 9/. In order to determine the stress levels we look at the volumetric strain.

By subtracting the elastic volumetric strain ε_{vol}^{e} from the total volumetric strain, a volumetric strain ε_{vol}^{cr} corresponding to the crack vol ume is obtained. This has been denoted calculated crack volumetric strain in the literature, cf. /8, 9/. We thus have

$$\varepsilon_{vol}^{cr} = \varepsilon_{vol} - \varepsilon_{vol}^{e}$$

Assuming axisymmetric loading, as in the triaxial compression test, and linear elasticity leads to

$$\varepsilon_{vol}^{cr} = \varepsilon_{vol} - \frac{1-2\nu}{E}(\sigma_a + 2\sigma_r)$$

Experimental investigations have shown that the crack initiation stress σ_i coincides with the onset of increase of the calculated crack volume, cf. /8, 9/. The same investigations also indicate that the crack damage stress σ_d can be defined as the axial stress at which the total volume starts to increase, i.e. when a dilatant behaviour is observed.

4.7 Nonconformities

The specimens aimed for the density and porosity measurements were first weighed with their natural water content and tested according to the method description SKB MD 160.002.

The specimens aimed for the mechanical tests were first subjected to hydrostatic loading and unloading and after that a triaxial compression test with constant confining pressure and axial deformation control. The initial hydrostatic compression load cycle and using axial deformation control at the triaxial compression tests are deviations from the method description SKB MD 190.003. Moreover, strain gauges were used for the deformation measurements, which are not recommended in the ISRM standard for triaxial testing /3/.

The specimens were tested according to the activity plan without departures.

5 Results

The results of the density and porosity measurements are presented in Section 5.1. The results from the mechanical tests of the individual specimens are presented in Section 5.2, and a summary of the results is given in Section 5.3. The reported parameters are based on unprocessed raw data obtained from the testing. One exception is the strain results that were adjusted due to a distortion caused by lateral pressure acting on the gauges. The results were reported to the SICADA database, where they are traceable by the activity plan number. Main results from the mechanical tests based on uncorrected strain measurement results are shown in Appendix A.

These data together with the digital photographs of the individual specimens were stored on a CD and handed over to SKB. The handling of the results follows SDP-508 (SKB internal controlling document) in general.

5.1 Density and porosity measurements

The results from the porosity and density determinations are shown in Tables 5-1 and 5-2. Diagrams showing the porosity and the density values versus sampling level are shown in Figures 5-1 and 5-2.

Table 5-1. Summary of results for porosity, dry density and wet density.

Identification	Porosity* (%)	Dry density (kg/m^3)	Density at natural moisture condition (kg/m^3)
KLX17A-80-1	0.37	2.763	2.767
KLX17A-80-2	0.46	2.756	2.760
KLX17A-80-4	0.39	2.672	2.676
KLX17A-80-5	0.48	2.673	2.678
KLX17A-80-7	0.34	2.688	2.691
KLX17A-80-8	0.32	2.686	2.689

* Note: The results are given with two significant digits. This has to be put in view of the calculated expanded uncertainty of ± 0.09% evaluated with a covering factor of two, cf. Section 3.2.

Table 5-2. Mean values and standard deviation of the results for porosity and density measurements.

	Porosity (%)	Dry density (kg/m^3)	Density at natural moisture condition (kg/m^3)
Mean value	0.39	2,706	2,710
Std dev	0.07	42	42

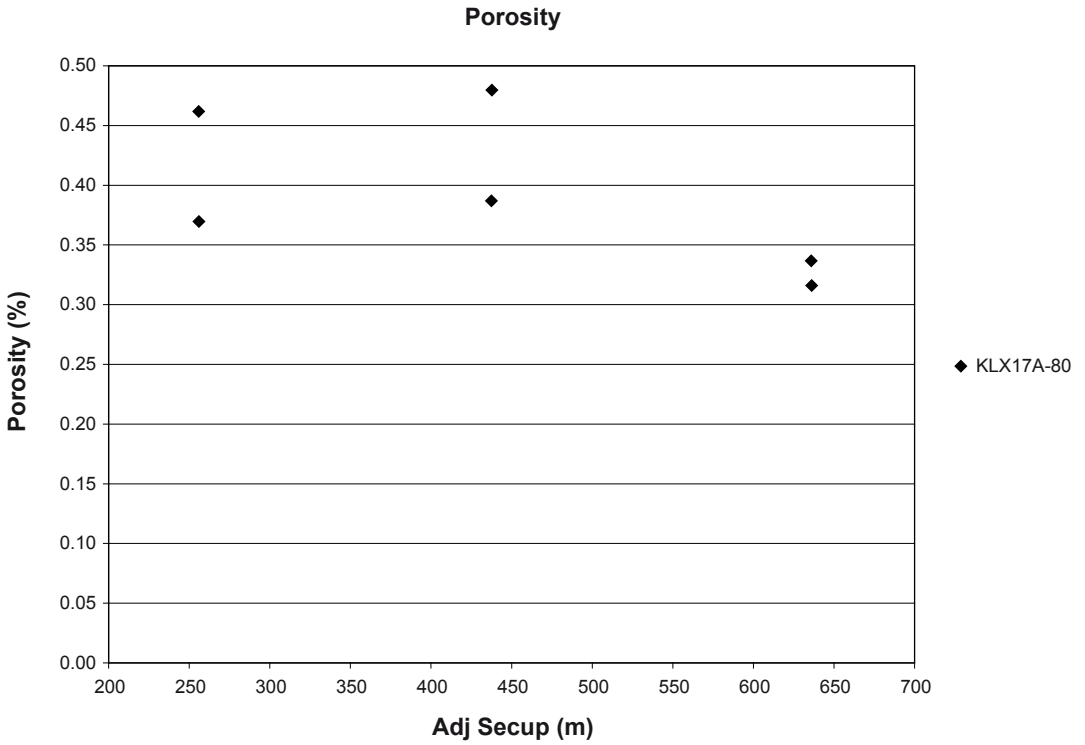

Figure 5-1. *Porosity versus sampling level (borehole length).*

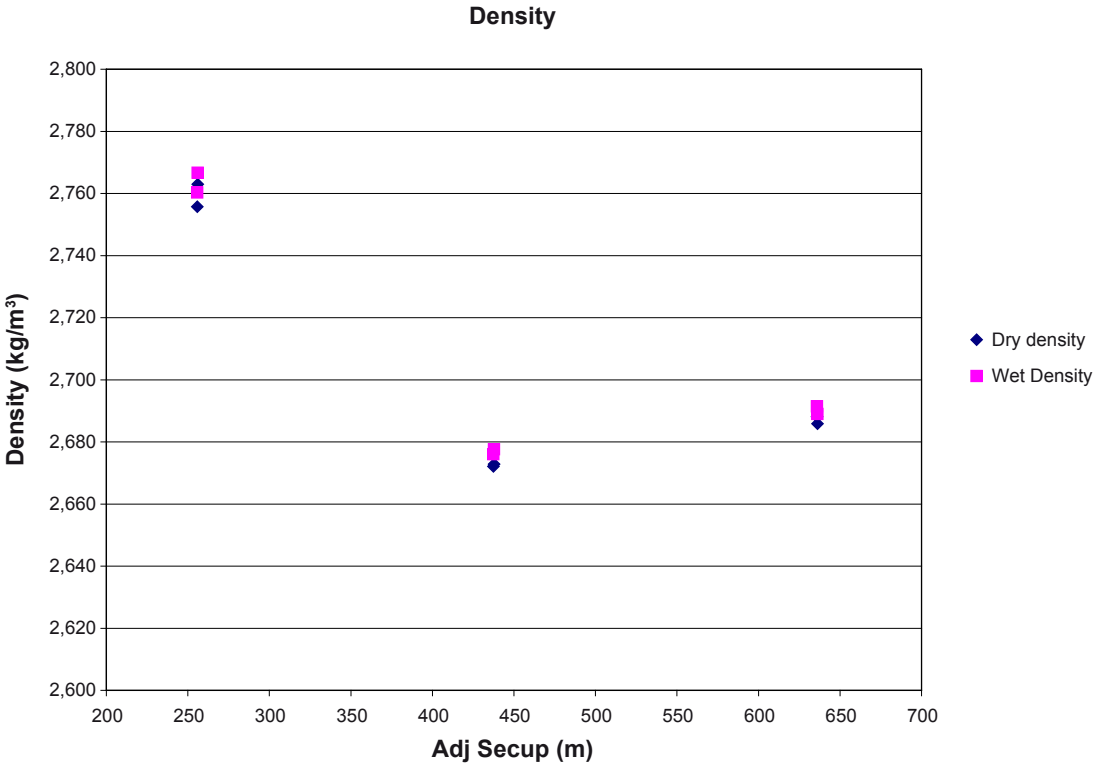

Figure 5-2. *Density versus sampling level (borehole length).*

5.2 Results from mechanical tests for each individual specimen

Pictures taken on the specimens before and after the mechanical test are presented below together with comments on observations made during testing. Results graphs from both the hydrostatic and triaxial compression tests are shown. The text “Based on all SGs” in the legend for the for the hydrostatic compression tests means that the results are computed using values from all strain gauges and evaluated according to equations (1)–(3) in Section 4-6. Moreover, the labels for strain gauges that have failed during the hydrostatic compression test are put between parenthesizes in the legends in the results diagrams. The strain results are adjusted with respect to the active lateral pressure according to Section 4.6. The results for the individual specimens are as follows:

Specimen ID: KLX17A-115-1

Before mechanical test

After mechanical test
AV, AH

BV, BH

CV, CH

Diameter (mm)	Height (mm)	Density (kg/m³)
50.1	126.8	2,760

Comments: A v-shaped shear failure is observed.

Specimen ID: KLX17A-115-1

Bulk compliance (β_{max}): 0.0164 [GPa^{-1}]

Microcrack volume (ε_{MC}): 0.011 [%]

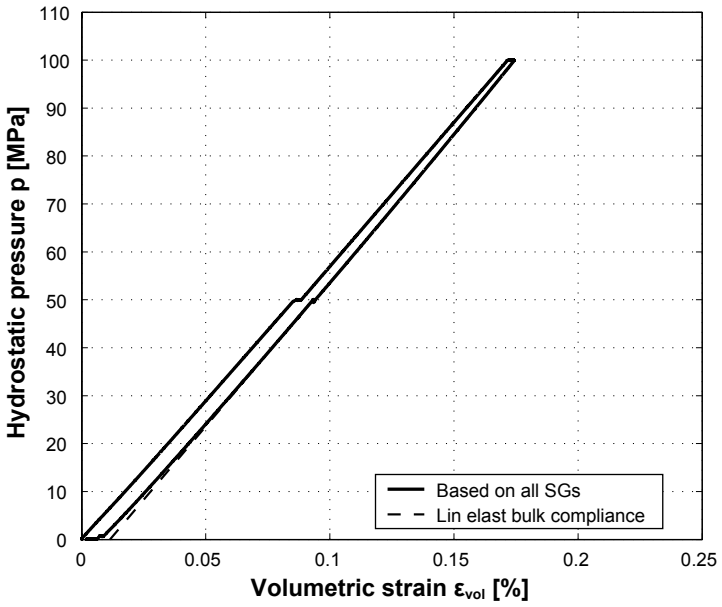

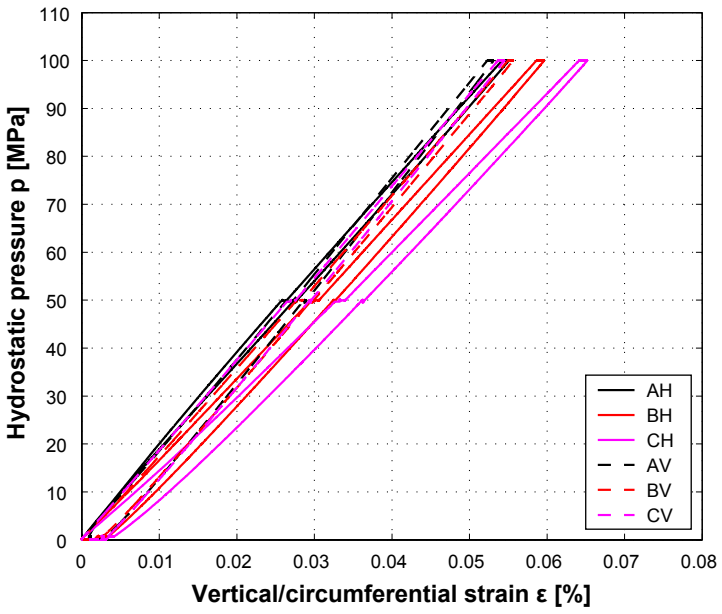

Specimen ID: KLX17A−115−1

Youngs Modulus (E):	71.7 [GPa]	Cell pressure:	10 [MPa]
Poisson Ratio (ν):	0.367 [−]		
Axial peak stress (σ_c):	292.6 [MPa]		

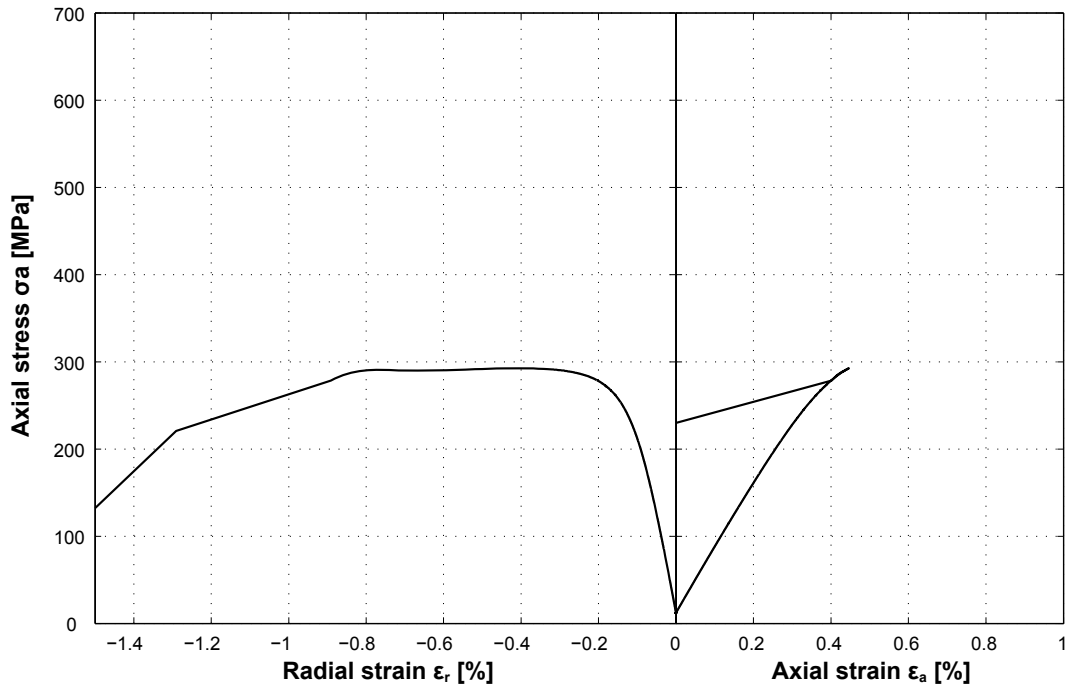

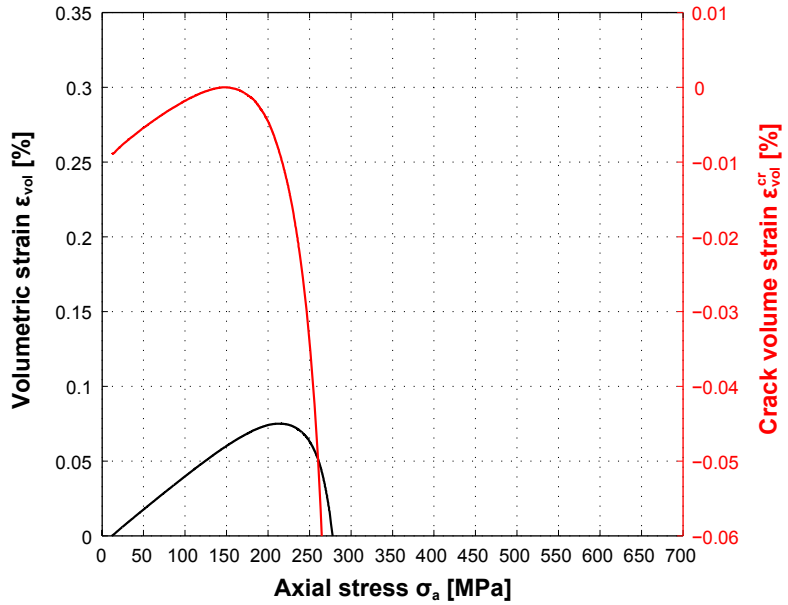

Specimen ID: KLX17A-115-2

Before mechanical test	After mechanical test AV, AH	BV, BH	CV, CH

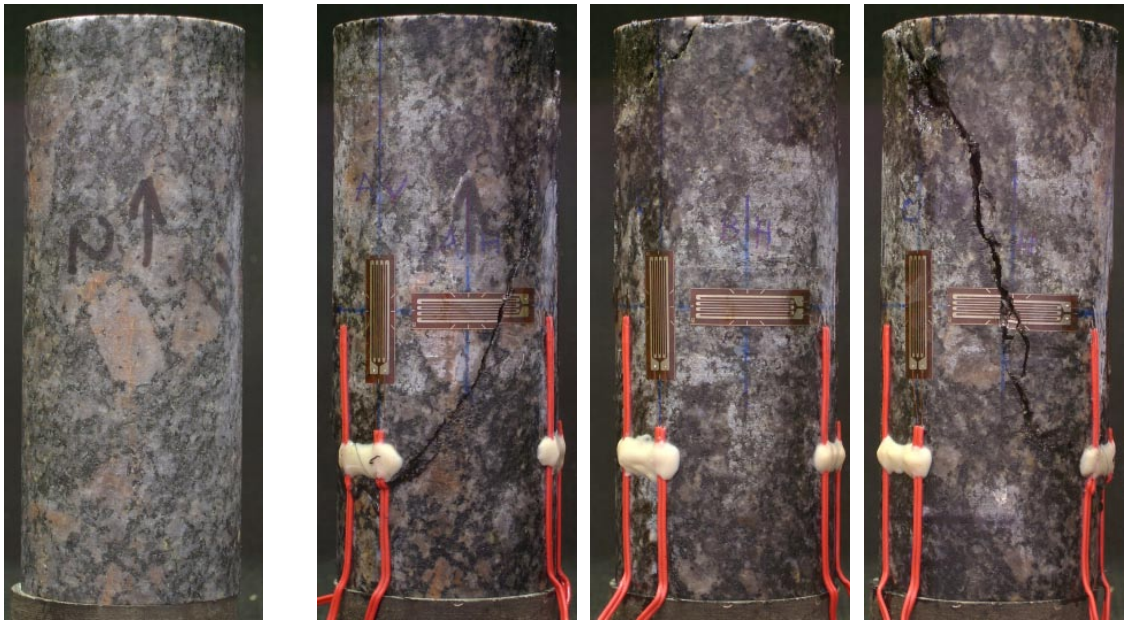

Diameter (mm)	Height (mm)	Density (kg/m^3)
50.1	127.1	2,770

Comments: A diagonal shear failure is observed.

Specimen ID: KLX17A-115-2

Bulk compliance (β_{max}): 0.0164 [GPa^{-1}]

Microcrack volume (ε_{MC}): 0.013 [%]

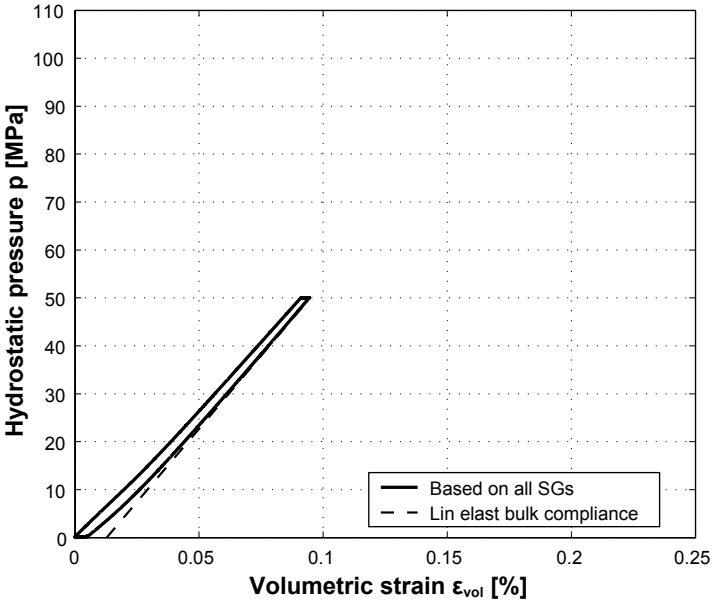

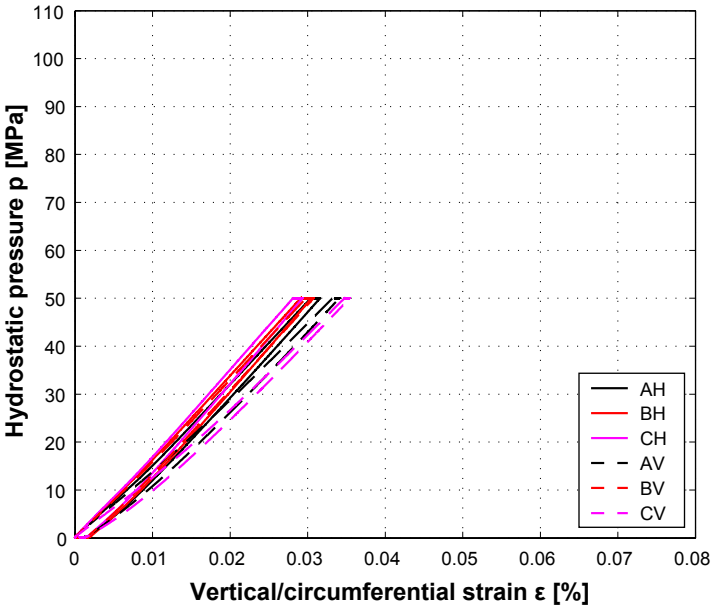

Specimen ID: KLX17A-115-2

Youngs Modulus (E):	65.1	[GPa]	Cell pressure:	50	[MPa]
Poisson Ratio (ν):	0.3	[–]			
Axial peak stress (σ_c):	493.1	[MPa]			

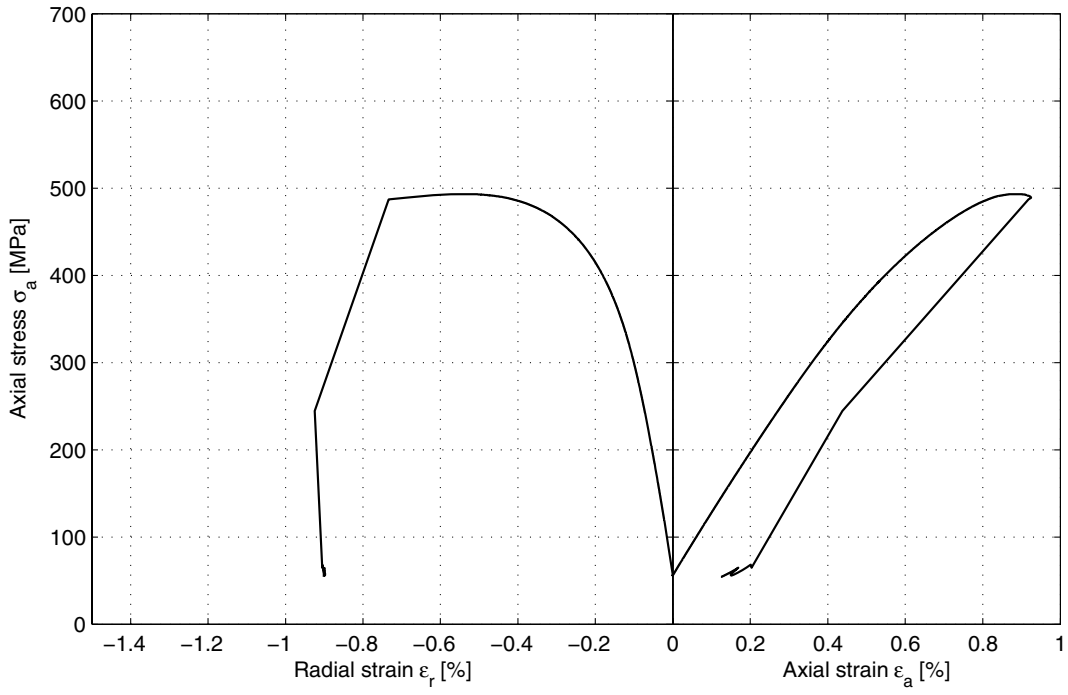

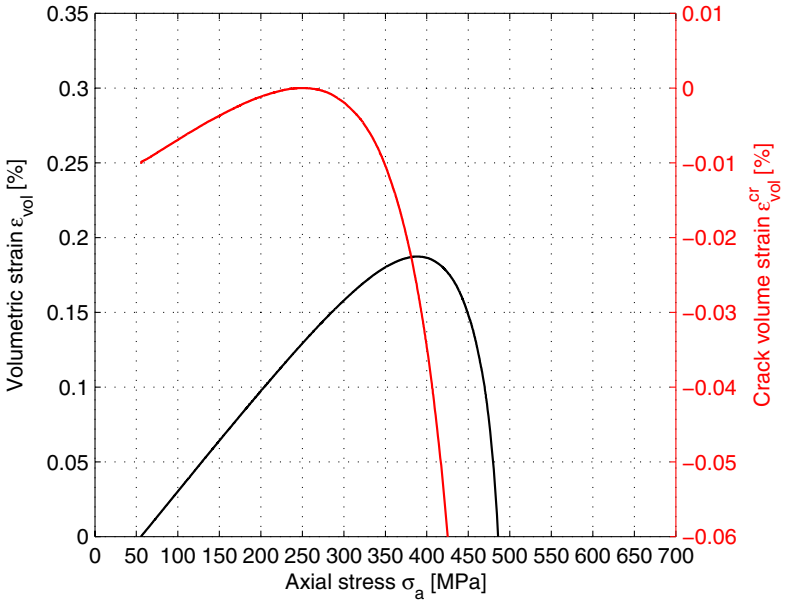

Specimen ID: KLX17A-115-4

Before mechanical test	After mechanical test AV, AH	BV, BH	CV, CH



Diameter (mm)	Height (mm)	Density (kg/m^3)
50.1	124.5	2,680

Comments: A v-shaped shear failure is observed.

Specimen ID: KLX17A–115–4

Bulk compliance (β_{max}): 0.02 [GPa^{-1}]

Microcrack volume (ε_{MC}): 0.028 [%]

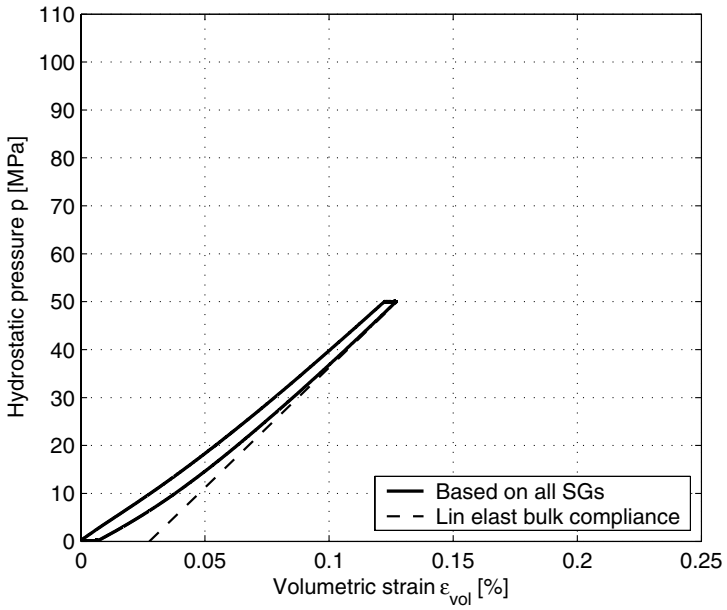

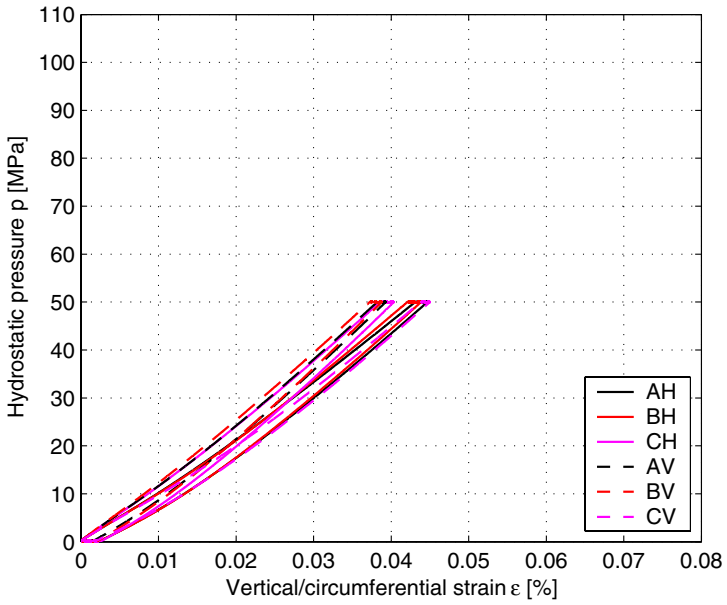

Specimen ID: KLX17A–115–4

Youngs Modulus (E):	69.6	[GPa]	Cell pressure:	10	[MPa]
Poisson Ratio (ν):	0.358	[–]			
Axial peak stress (σ_c):	321	[MPa]			

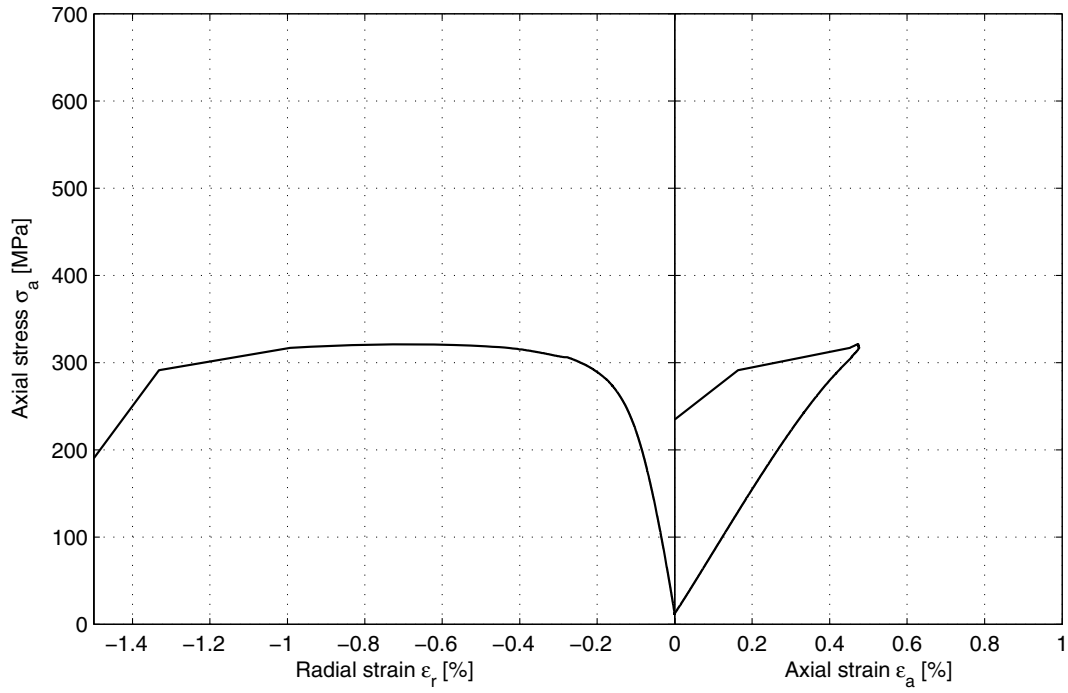

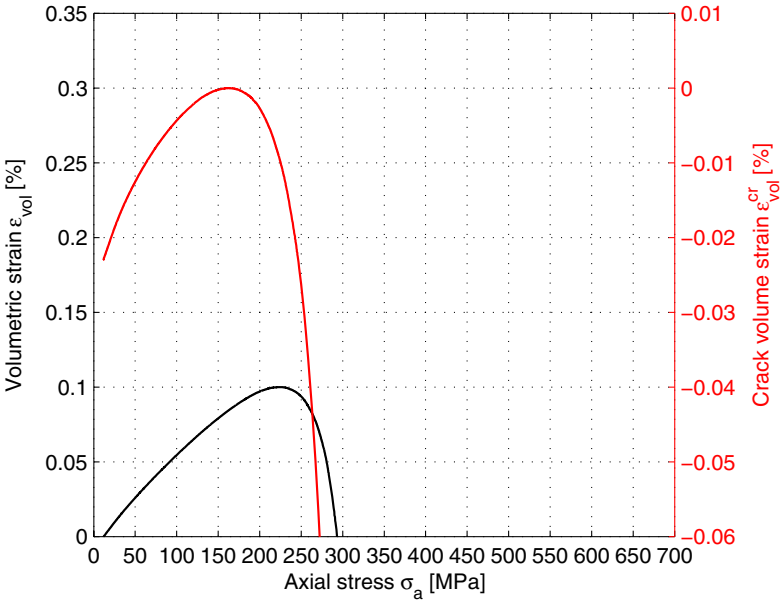

Specimen ID: KLX17A-115-5

Before mechanical test	After mechanical test AV, AH	BV, BH	CV, CH

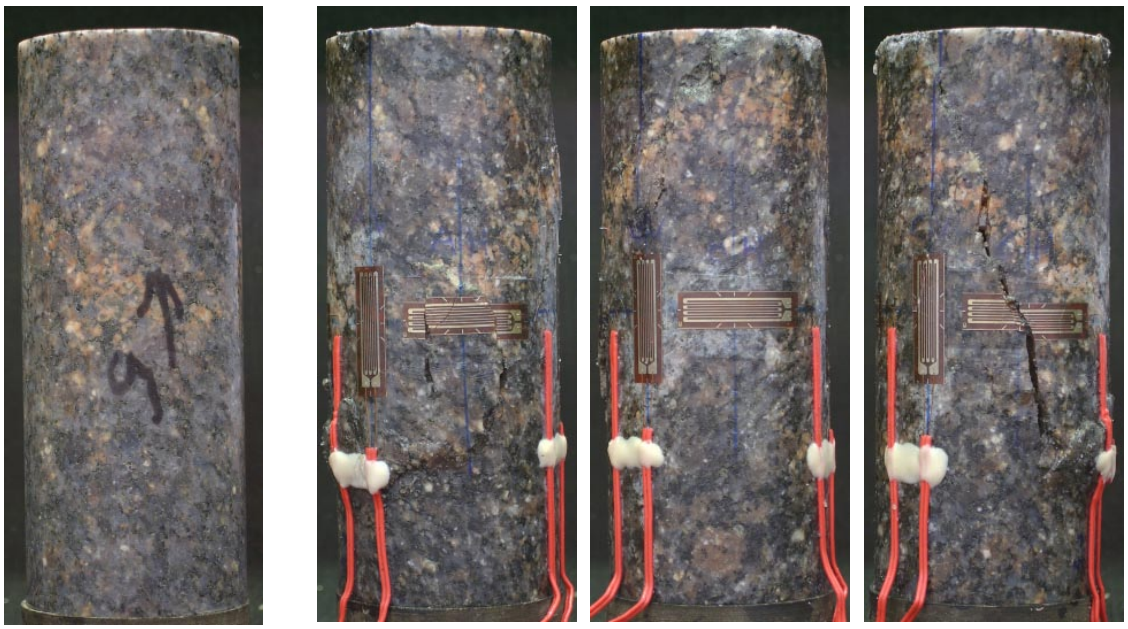

Diameter (mm)	Height (mm)	Density (kg/m^3)
50.1	126.4	2,680

Comments: The specimen has a diagonal shear failure.

Specimen ID: KLX17A–115–5

Bulk compliance (β_{max}): 0.0198 [GPa^{-1}]

Microcrack volume (ε_{MC}): 0.027 [%]

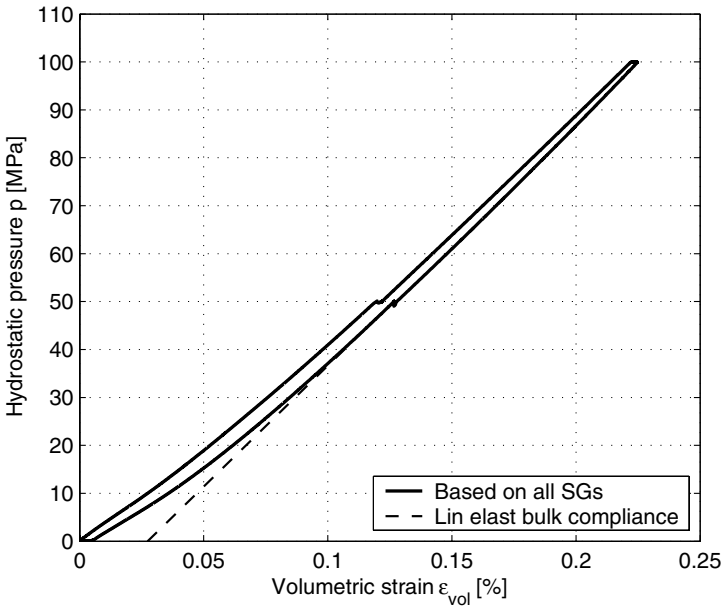

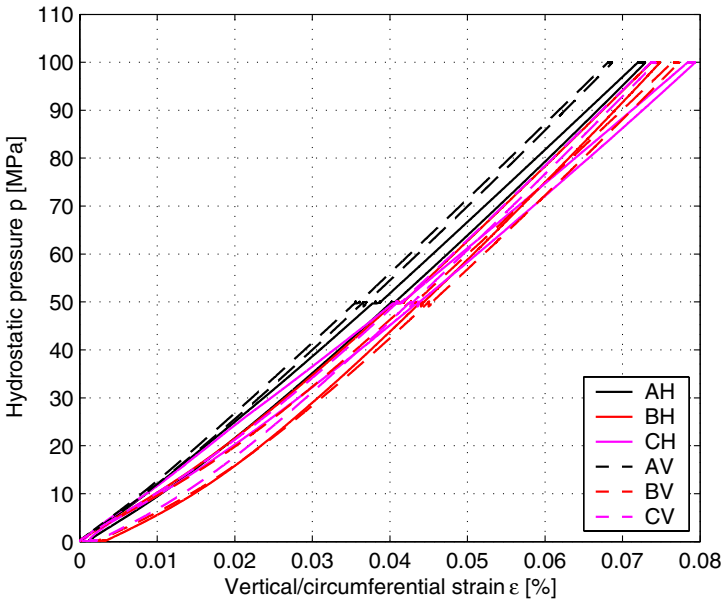

Specimen ID: KLX17A−115−5

Youngs Modulus (E):	66.9	[GPa]	Cell pressure:	49	[MPa]
Poisson Ratio (ν):	0.299	[–]			
Axial peak stress (σ_c):	580.1	[MPa]			

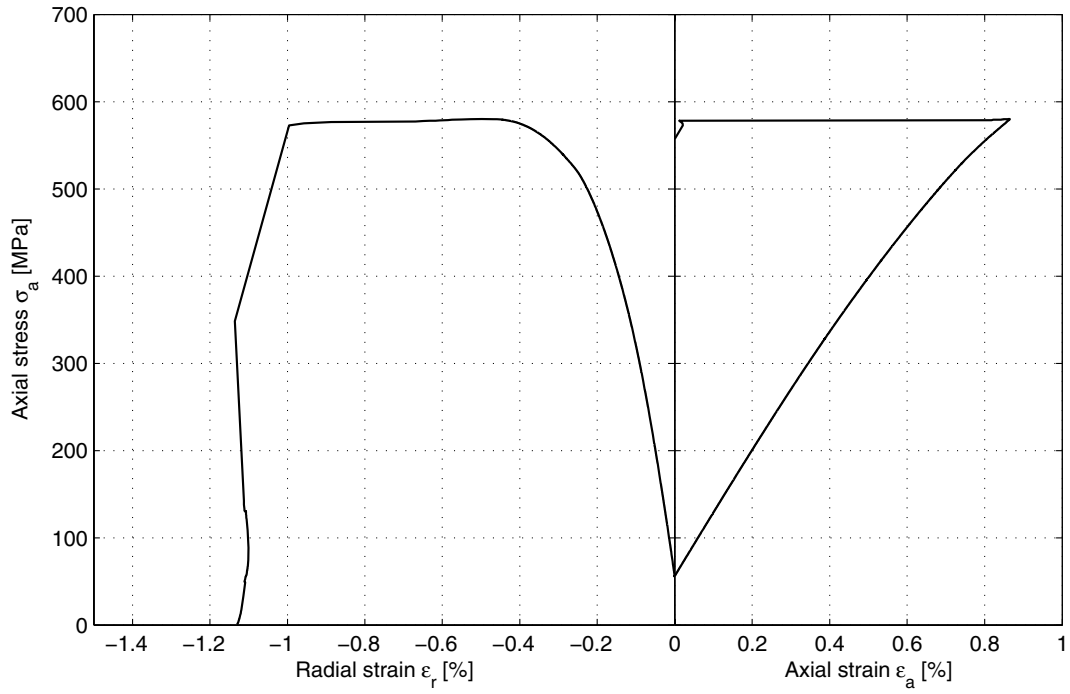

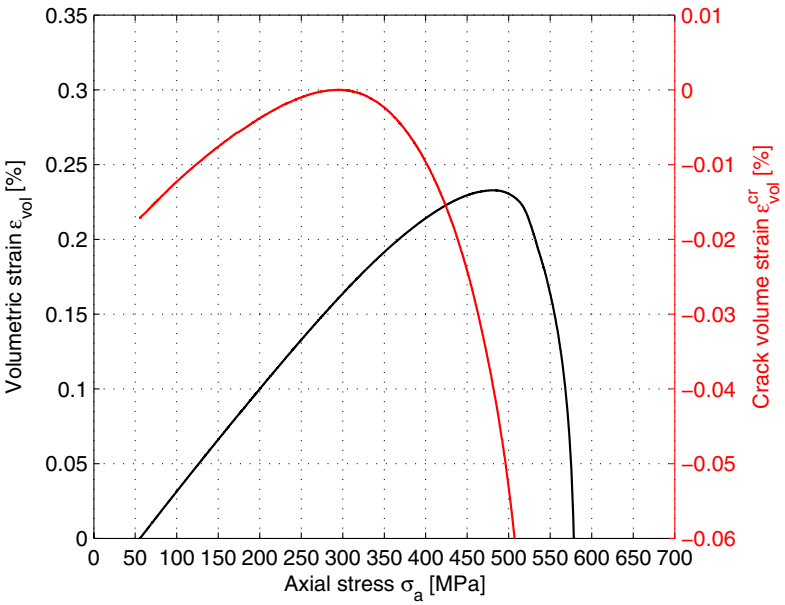

Specimen ID: KLX17A-115-7

Before mechanical test	After mechanical test AV, AH	BV, BH	CV, CH

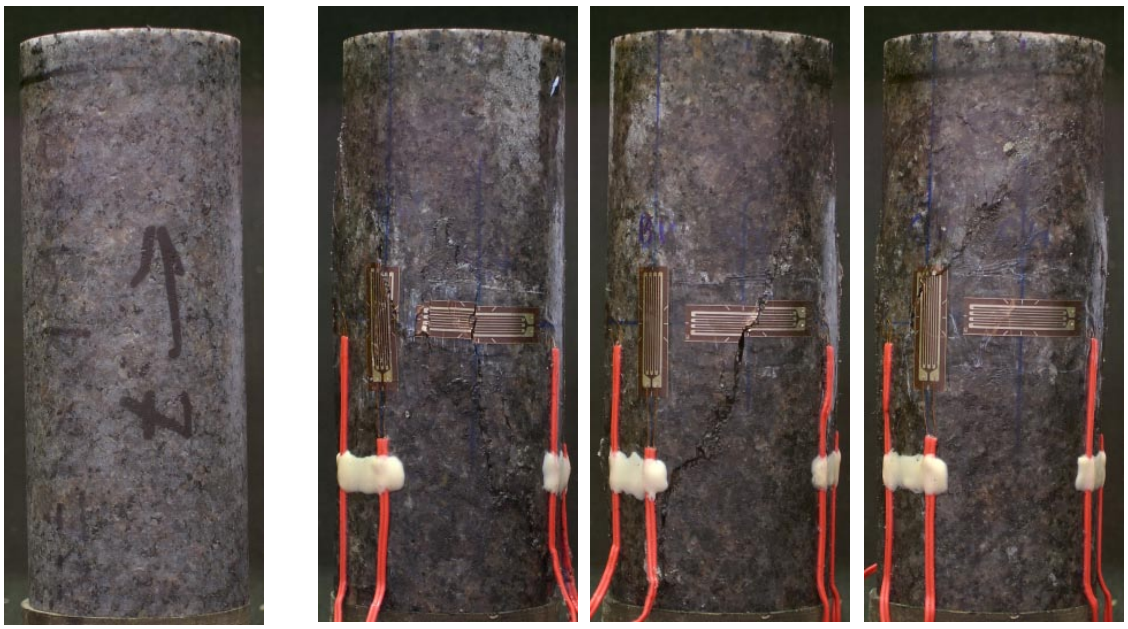

Diameter (mm)	Height (mm)	Density (kg/m^3)
49.9	126.3	2,690

Comments: The specimen has a diagonal shear failure.

Specimen ID: KLX17A–115–7

Bulk compliance (β_{max}): 0.0202 [GPa^{-1}]

Microcrack volume (ε_{MC}): 0.048 [%]

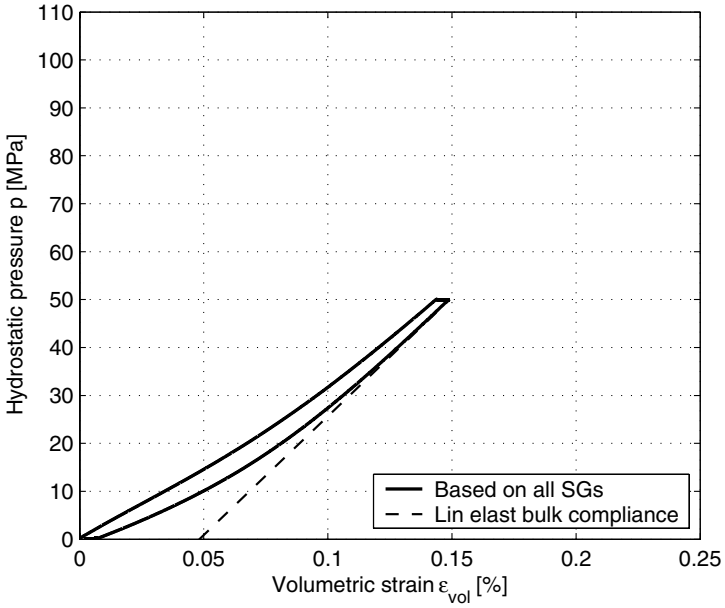

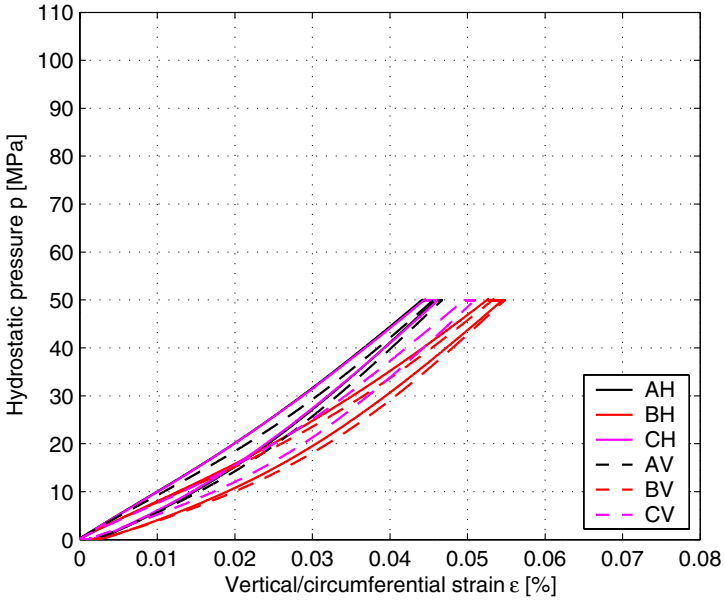

Specimen ID: KLX17A−115−7

Youngs Modulus (E):	68.2	[GPa]	Cell pressure:	10	[MPa]
Poisson Ratio (ν):	0.353	[–]			
Axial peak stress (σ_c):	301.2	[MPa]			

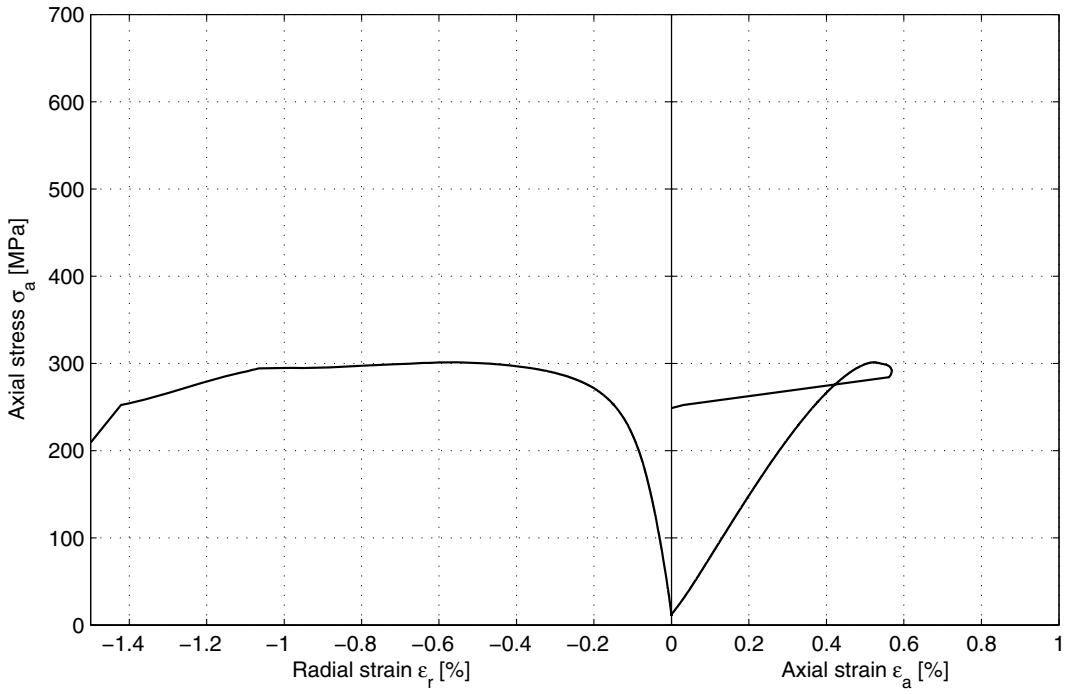

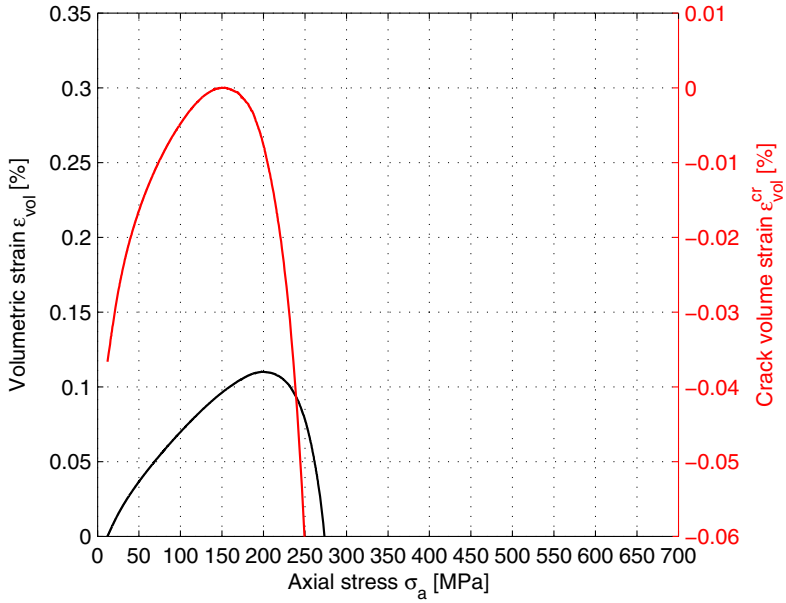

Specimen ID: KLX17A-115-8

Before mechanical test	After mechanical test AV, AH	BV, BH	CV, CH

Diameter (mm)	Height (mm)	Density (kg/m³)
49.9	126.3	2,690

Comments: Strain gauge AV has failed during the measurement. The measured strain ε_{AV} has been replaced by the mean value of the strains measured by the strain gauges BV and CV in the volumeteric strain calculation, i.e. $\varepsilon_{AV} = (\varepsilon_{BV} + \varepsilon_{CV}) / 2$. The specimen has a diagonal shear failure.

Specimen ID: KLX17A–115–8

Bulk compliance (β_{max}): 0.0192 [GPa^{-1}]

Microcrack volume (ε_{MC}): 0.027 [%]

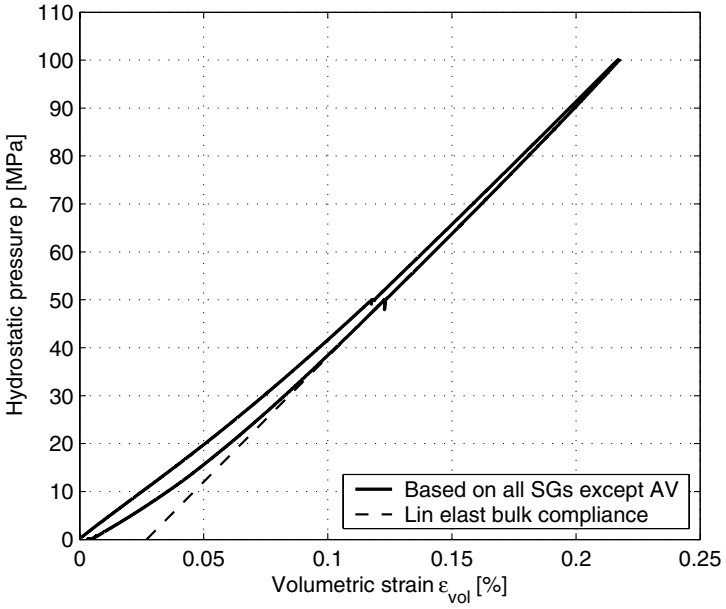

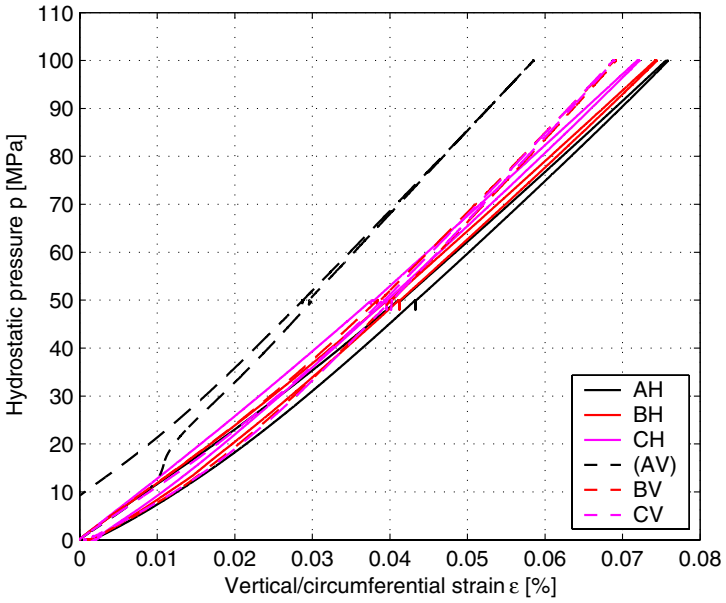

Specimen ID: KLX17A−115−8

Youngs Modulus (E):	72.7	[GPa]	Cell pressure:	50	[MPa]
Poisson Ratio (ν):	0.311	[–]			
Axial peak stress (σ_c):	508.7	[MPa]			

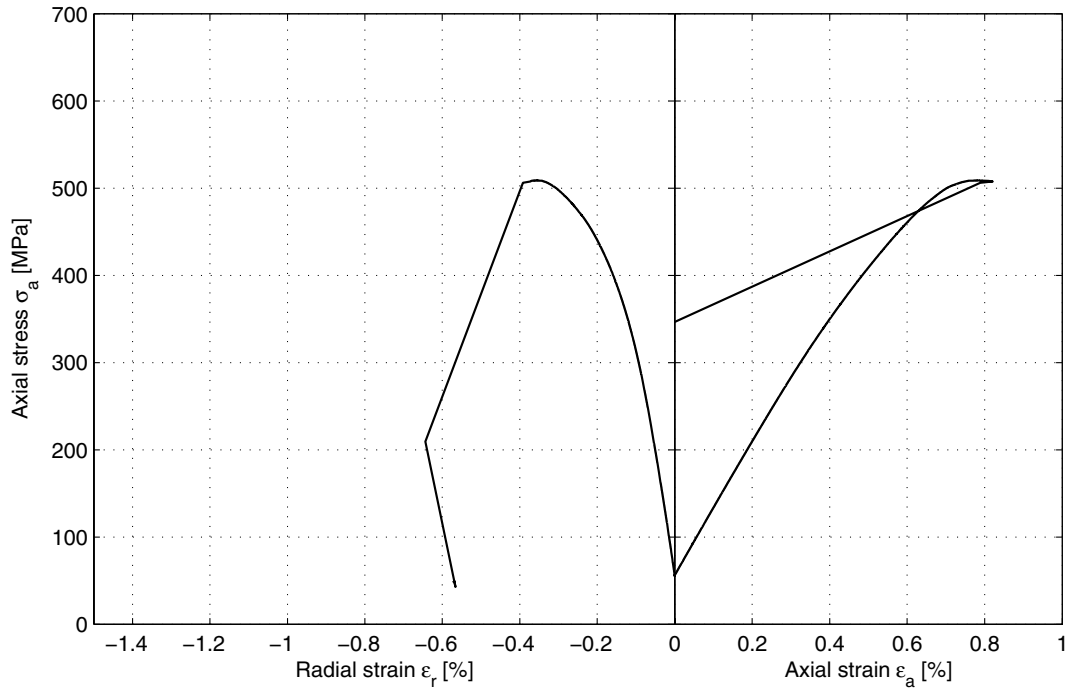

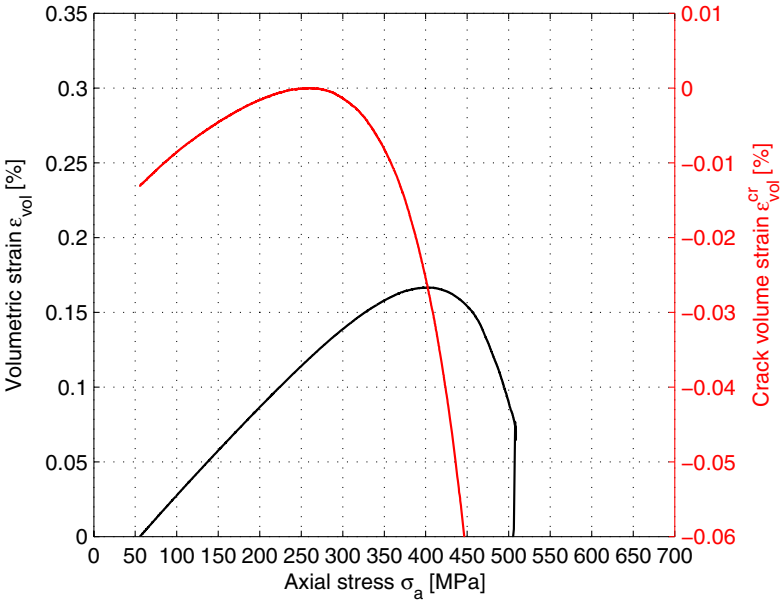

5.3 Summary of results from the mechanical tests

A summary of results from the mechanical tests is shown in Tables 5-3 and 5-4. The microcrack volume, density, triaxial compressive strength, the tangent Young's modulus and the tangent Poisson ratio versus sampling level (borehole length), are presented in Figures 5-3 to 5-7. The results are based on adjusted data from the strain measurements. Results based on strain data without the lateral pressure correction are shown in Appendix A.

Table 5-3. Summary of results.

Identification	Hydrostatic compr tests			Triaxial compression tests				
	β_{max} (GPa^{-1})	ε_{MC} (%)	$\varepsilon_{vol,20}$ (%)	Conf press (MPa)	Density (kg/m^3)	Compressive strength (MPa)	Young's modulus (GPa)	Poisson ratio (–)
KLX17A-115-1	0.0164	0.011	0.043	10	2,760	292.6	71.7	0.37
KLX17A-115-2	0.0164	0.013	0.044	50	2,770	493.1	65.1	0.30
KLX17A-115-4	0.0200	0.028	0.063	10	2,680	321.0	69.6	0.36
KLX17A-115-5	0.0198	0.027	0.062	50	2,680	580.1	66.9	0.30
KLX17A-115-7	0.0202	0.048	0.081	10	2,690	301.2	68.2	0.35
KLX17A-115-8	0.0192	0.027	0.060	50	2,690	508.7	72.7	0.31

Table 5-4. Calculated mean values and standard deviation.

	Density (kg/m^3)	Young's modulus (GPa)	Poisson ratio (–)
Mean value	2,712	69.0	0.33
Std dev	42	2.9	0.03

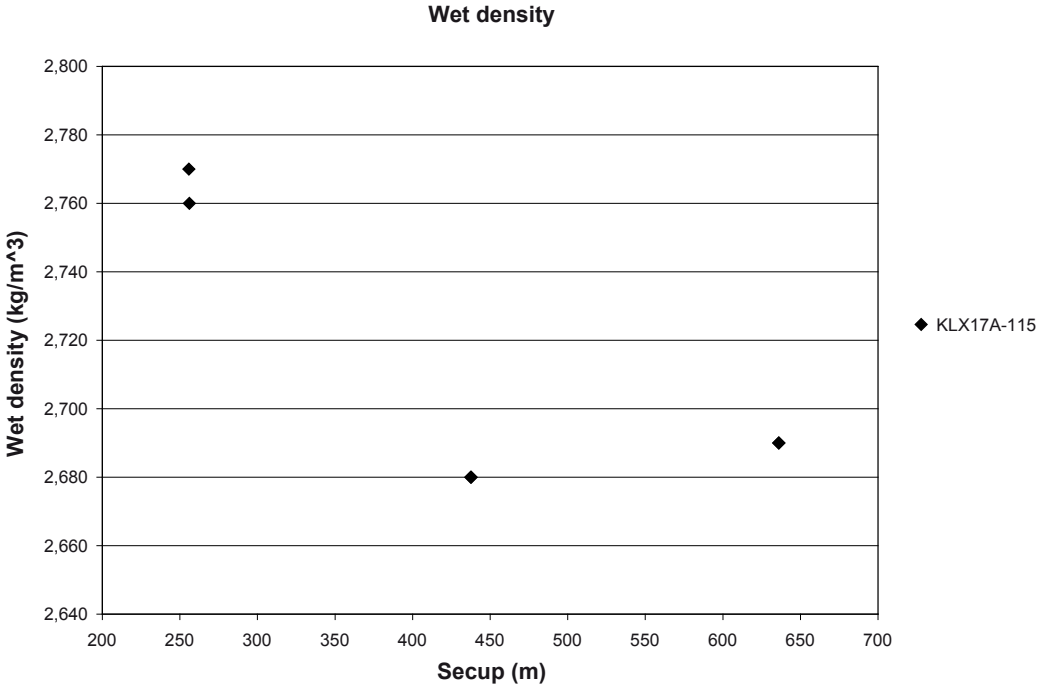

Figure 5-3. *Density versus sampling level (borehole length).*

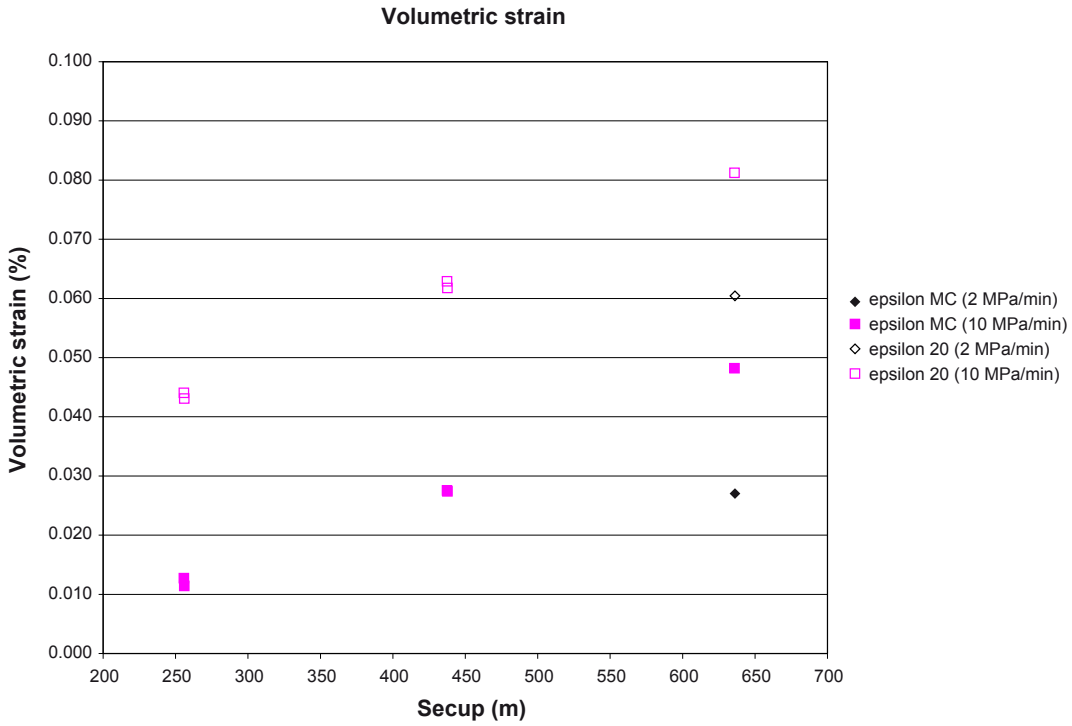

Figure 5-4. *Microcrack volume versus sampling level (borehole length).*

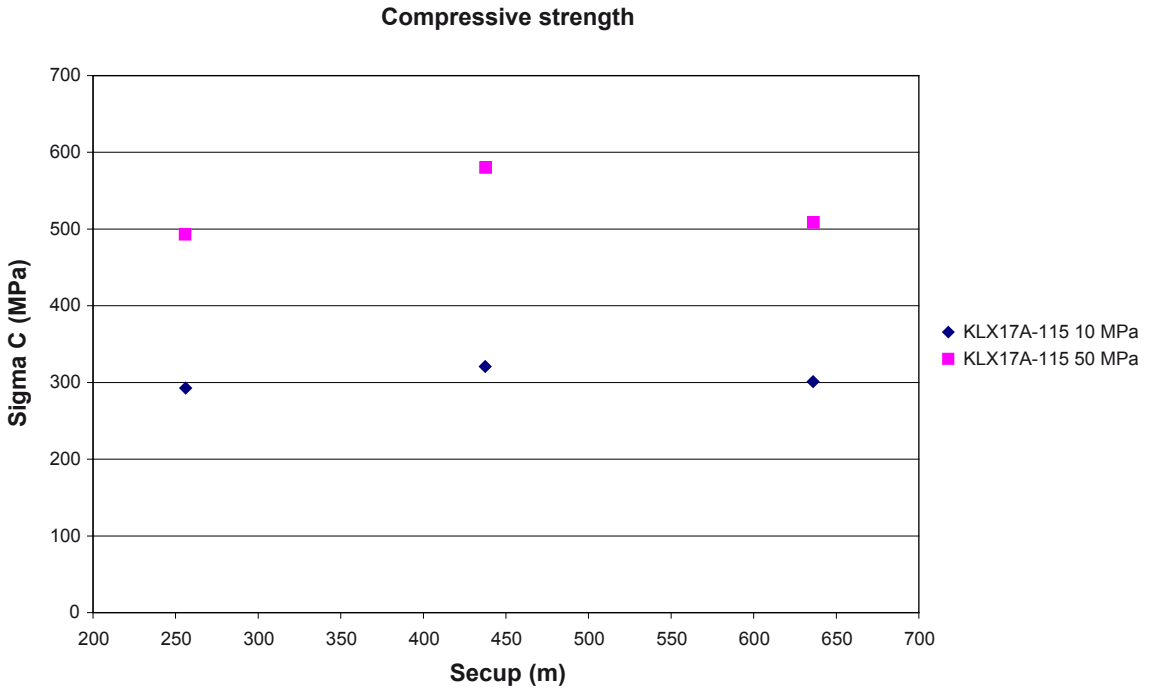

Figure 5-5. *Compressive strength versus sampling level (borehole length).*

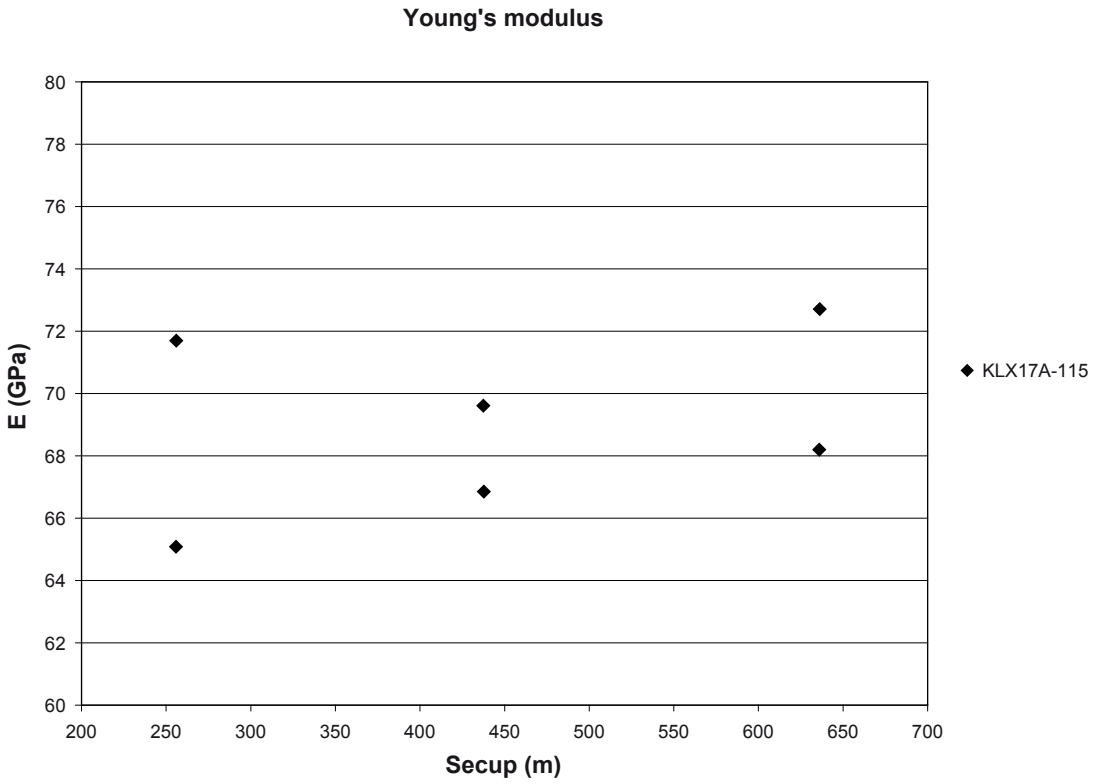

Figure 5-6. *Tangent Young's modulus versus sampling level (borehole length).*

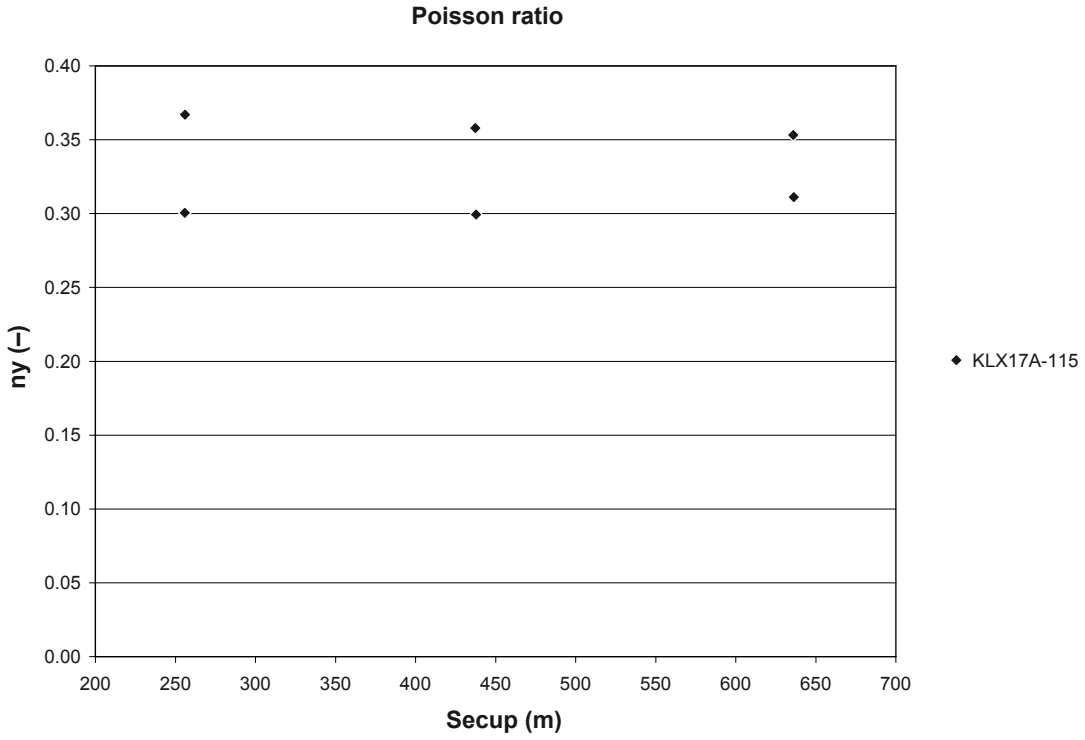

Figure 5-7. *Tangent Poisson ratio versus sampling level (borehole length).*

5.4 Discussion of results

The results of the porosity measurement display a value of 0.37–0.48% at the 250 m and 430 m depth levels and slightly lower namely 0.32–0.34% at the 630 m depth level, see Table 5-1. As to the density measurements, the density is c 2,760 kg/m^3 at the 250 m depth level as compared with c 2,680 kg/m^3 and c 2,690 kg/m^3 at the 430 m and 630 m depth levels, respectively.

The five first specimens, KLX17A-115-1 to KLX17A-115-7, were loaded up to 50 MPa, respectively 100 MPa, during the hydrostatic compression tests with a rate of 10 MPa/min during loading and unloading with a hold time of 15 minutes at full loading. The last specimen KLX17A-115-8 was loaded up to 100 MPa but with a decreased loading rate of 2 MPa/min and a short hold time. There seems to be a tendency that the microcrack volume (ε_{MC}), bulk compliance (β_{max}) as well as the volumetric strain at 20 MPa (ε_{20}) increase with depth, cf. Table 5-3 and in Figure 5-4. The tendency is a rather linear relationships with depth level if the results from the tests with 10 MPa/min loading rate are considered. The results from the test with 2 MPa/min at the 630 m depth level display values as compared with the corresponding results with the 10 MPa/min loading rate at the same depth level. This might indicate a dependency on the loading rate. However, as only one specimen was tested with the lower loading rate makes the observation difficult to conclude.

A number of factors affect the outcome of the tests for the determination of the microcrack volume and are important to understand for the interpretation of the results. However, it is difficult at this stage to determine the impact on the test results of each one of the parameters without further investigations. They can be related to the specimens or to the test method. Some circumstances that make a difference in history between the specimens are listed below without order of significance and without further elaborations:

- The rock type can vary with sampling depth.
- The history of in situ rock stresses and the in situ stress state at the time of sampling.
- The actual choice of drill equipment can affect the magnitude of the mechanical forces acting on the cores during the drilling.
- The storage time after sampling in a stress relieved condition.
- Water content in the specimens. The water content may influence the closing of the microcracks during compression. For example, various conditions may be dried during storage, dried during storage and water saturated by immersion or fresh specimens with preserved natural water content.

The results of the tests are dependent on how the tests were conducted and how the results have been extracted, which contribute to the total measurement error. Some of the contributing parts are listed below:

- The loading rate may influence the closing of the microcracks as indicated above.
- Some of the specimens were loaded up to 100 MPa in order to have results clearly within the pressure threshold which corresponds to full closure of stress induced microcracks, cf. Figure 4-1.
- The tangent value of the bulk compliance was evaluated at the unloading path at a pressure level of 50 MPa. A linear elastic bulk response was assumed when no stress induced microcracks were present. The microcrack volume strain was computed according to (4), cf. Figure 4-1. This approximation yields a model error, which is dependent on the deviation from linearity of the true elastic bulk response and on the amount of the hysteresis, which affects the evaluation of the tangent bulk compliance (β_{max}). It can be observed that the real response display a slight non-linearity within the pressure range which is above the limit for the closure of stress induced microcracks.

Further investigations may concern the effect of various types of sampling procedure. For example the time of storage in a stress relaxed condition or drying of the specimens can be investigated. Furthermore, it is reasonable to believe that recently drilled cores which have not dried should preferable be used in the tests in order to eliminate the questions about effect of the storage. Moreover, other investigations may concern evaluation of the model error of the linearity approximation of the bulk response. Moreover, more tests with a low loading rate, e.g. 2 MPa/min can be used to confirm a possible rate effect in the closure of microcracks and volumetric response.

References

/1/ **SKB, 2001.** Site investigations. Investigation methods and general execution programme. SKB TR-01-29, Svensk Kärnbränslehantering AB.

/2/ **ISRM, 1979.** Suggested Method for Determining Water Content. Porosity, Density, Absorption and Related Properties and Swelling and Slake-durability Index Properties, Int. J. Rock. Mech. Min. Sci. & Geomech. Abstr. 16(2), pp. 141–156.

/3/ **ISRM, 1983.** Suggested method for determining the strength of rock material in triaxial compression: Revised version, Int. J. Rock. Mech. Min. Sci. & Geomech. Abstr. 20(6), pp. 283–290.

/4/ **ISRM, 1999.** Draft ISRM suggested method for the complete stress-strain curve for intact rock in uniaxial compression, Int. J. Rock. Mech. Min. Sci. 36(3), pp. 279–289.

/5/ **Jacobsson L, 2007.** Forsmark site investigation, boreholes KFM01A and KFM02B. Microcrack volume measurements and triaxial compression test on intact rock. SKB P-07-93, Svensk Kärnbränslehantering AB.

/6/ **Brace W F, 1965.** Some new measurements of linear compressibility of rocks, J. Geophys. Res. 70(2), pp. 391–398.

/7/ **Walsh J B, 1965.** The effect of cracks on the compressibility of rock, J. Geophys. Res. 70(2), pp. 381–389.

/8/ **Martin C D, Chandler N A, 1994.** The progressive fracture of Lac du Bonnet granite, Int. J. Rock. Mech. Min. Sci. Geomech. Abstr. 31(6), pp. 643–659.

/9/ **Eberhardt E, Stead D, Stimpson B, Read R S, 1998.** Identifying crack initiation and propagation thresholds in brittle rock. Can. Geotech. J. 35, pp. 222–233.

/10/ **ASTM 4543-01, 2001.** Standard practice for preparing rock core specimens and determining dimensional and shape tolerance.

/11/ **Savukoski M, 2006.** Oskarshamn site investigation, drill hole KLX12A. Determination of porosity by water saturation and density by buoyancy technique, SKB P-06-71, Svensk Kärnbränslehantering AB.

/12/ **Hoffman K, 1989.** An introduction to measurements using strain gages. Hottinger Baldwin Messtechnik GmbH, Darmstadt.

/13/ **Brace W F, 1964.** Effect of pressure on electrical resistance strain gages, Exp. Mech 4, pp 212–216.

/14/ **Lau J S O, Chandler N A, 2004.** Innovative laboratory testing, Int. J. Rock. Mech Sci. 41(8), pp. 1427–1445.

/15/ **Stråhle A, 2001.** Definition och beskrivning av parametrar för geologisk, geofysisk och bergmekanisk kartering av berg. SKB R-01-19, Svensk Kärnbränslehantering AB.

/16/ **MATLAB, 2002.** The Language of Technical computing. Version 6.5. MathWorks Inc.

Appendix A

Results from mechanical tests without lateral pressure correction

Results based on strain measurements in which no adjustment for the effect of lateral pressure are shown below in Tables A-1 to A-2.

Table A-1. Summary of results based on original strain data.

Identification	Hydrostatic compr tests			Triaxial compression tests				
	β_{max} (GPa^{-1})	ε_{MC} (%)	$\varepsilon_{vol,20}$ (%)	Conf press (MPa)	Density (kg/m^3)	Compressive strength (MPa)	Young's modulus (GPa)	Poisson ratio (–)
KLX17A-115-1	0.0154	0.011	0.041	10	2,760	292.6	71.7	0.37
KLX17A-115-2	0.0154	0.013	0.042	50	2,770	493.1	65.1	0.30
KLX17A-115-4	0.0190	0.028	0.061	10	2,680	321.0	69.6	0.36
KLX17A-115-5	0.0189	0.027	0.060	50	2,680	580.1	66.9	0.30
KLX17A-115-7	0.0192	0.048	0.079	10	2,690	301.2	68.2	0.35
KLX17A-115-8	0.0182	0.027	0.059	50	2,690	508.7	72.7	0.31

Table A-2. Calculated mean values and standard deviation based on original strain data.

	Density (kg/m^3)	Young's modulus (GPa)	Poisson ratio (–)
Mean value	2,712	69.0	0.33
Std dev	42	2.9	0.03